TKK Dissertations 78
Espoo 2007

MAGNETIC AND MAGNETO-MECHANICAL PROPERTIES OF Ni-Mn-Ga MAGNETIC SHAPE MEMORY ALLOYS

Doctoral Dissertation

Ladislav Straka

Helsinki University of Technology
Department of Engineering Physics and Mathematics
Laboratory of Biomedical Engineering

TKK Dissertations 78
Espoo 2007

MAGNETIC AND MAGNETO-MECHANICAL PROPERTIES OF Ni-Mn-Ga MAGNETIC SHAPE MEMORY ALLOYS

Doctoral Dissertation

Ladislav Straka

Dissertation for the degree of Doctor of Science in Technology to be presented with due permission of the Department of Engineering Physics and Mathematics for public examination and debate in Auditorium F1 at Helsinki University of Technology (Espoo, Finland) on the 15th of June, 2007, at 12 noon.

Helsinki University of Technology
Department of Engineering Physics and Mathematics
Laboratory of Biomedical Engineering

Teknillinen korkeakoulu
Teknillisen fysiikan ja matematiikan osasto
Lääketieteellisen tekniikan laboratorio

Distribution:
Helsinki University of Technology
Department of Engineering Physics and Mathematics
Laboratory of Biomedical Engineering
P.O. Box 2200 (Rakentajanaukio 2 C)
FI - 02015 TKK
FINLAND
URL: http://biomed.tkk.fi/
Tel. +358-(0)9-451 3172
Fax +358-(0)9-451 3182
E-mail: ladislav.straka@tkk.fi

ISBN 978-951-22-8819-9
ISBN 978-951-22-8820-5 (PDF)
ISSN 1795-2239
ISSN 1795-4584 (PDF)
URL: http://lib.tkk.fi/Diss/2007/isbn9789512288205/

TKK-DISS-2312

Valopaino Oy
Helsinki 2007

ABSTRACT OF DOCTORAL DISSERTATION	HELSINKI UNIVERSITY OF TECHNOLOGY P. O. BOX 1000, FI-02015 TKK http://www.tkk.fi

Author Ladislav Straka

Name of the dissertation

Magnetic and Magneto-Mechanical Properties of Ni-Mn-Ga Magnetic Shape Memory Alloys

Manuscript submitted 6.2.2007	Manuscript revised 22.5.2007
Date of the defence 15.6.2007	
☐ Monograph	☒ Article dissertation (summary + original articles)
Department	Department of Engineering Physics and Mathematics
Laboratory	Laboratory of Biomedical Engineering
Field of research	Magnetic shape memory alloys
Opponent(s)	Professor Gregory Carman
Supervisor	Professor Ari Koskelainen
Instructor	Dr. Oleg Heczko

Abstract

Ni-Mn-Ga alloys close to stoichiometric $Ni_{50}Mn_{25}Ga_{25}$ (at. %) composition have recently gained considerable interest due to the possibility of rearrangement of their martensite microstructure in magnetic field. The rearrangement is accompanied by large strains of up to 10%. This effect is different from ordinary magnetostriction and it is referred to as magnetic shape memory effect (MSME).

The Thesis presents the first attempt to study the temperature limits of irreversible and reversible MSME by exploiting a theoretical model and experimentally determined temperature dependences of magnetic and other material properties governing the existence of MSME. The obtained predictions are compared with direct observations of MSME. Extraordinary magneto-mechanical effects in Ni-Mn-Ga alloys, not discussed previously, are investigated and compared with theoretical models in this Thesis. These effects include reversible MSME with strain close to 6%, magnetic field controlled superelasticity with strain close to 6%, and up to 30% changes of magnetization during loading in static magnetic field. Unique simultaneous measurements of strain and magnetization on Ni-Mn-Ga alloys are presented for various experiments such as, e.g., during MSME and reversible MSME.

The broad spectrum of experiments presented in the Thesis corroborates the important role of magnetic anisotropy, twinning stress and temperature for existence and reversibility of MSME. The simultaneous measurement of strain and magnetization in various experiments confirms experimentally the close relation between martensite microstructure and its magnetic properties and demonstrates the interplay between martensite microstructure and magnetic field. Good agreement of all presented experimental results with the used theoretical model supports validity of the model and shows that the model is suitabile for predicting temperature and stress limits of MSME or reversible MSME, and for modelling of magnetic-field induced superelasticity. Some of the presented experiments can additionally be considered as application examples. The original findings presented in this Thesis broaden the general scientific understanding of MSME and can serve as informative source when considering possible engineering usage of Ni-Mn-Ga alloys as actuators, sensors, or intelligent material.

Keywords Ni-Mn-Ga, martensite, magnetic shape memory, temperature dependence	
ISBN (printed) 978-951-22-8819-9	ISSN (printed) 1795-2239
ISBN (pdf) 978-951-22-8820-5	ISSN (pdf) 1795-4584
Language English	Number of pages 68p. + app. 44p.
Publisher Laboratory of Biomedical Engineering	
Print distribution Laboratory of Biomedical Engineering	
☒ The dissertation can be read at http://lib.tkk.fi/Diss/2007/isbn9789512288205/	

Preface

I got in touch with the magnetic shape memory alloys for the first time during my short employment in MSM-project in Laboratory of Physical Metallurgy and Materials Science in Helsinki University of Technology in 2000. As I considered the topic to be quite interesting I continued in the same project in Laboratory of Biomedical Engineering in Helsinki University of Technology during 2001–2004. However, the MSM-project ended in 2004. I tried to continue the work, although I was simultaneously occupied with different topics and new duties in Laboratory of Engineering Materials in Helsinki University of Technology. Now, after almost six years, my Thesis are finished.

At first, I would like to express my greatest gratitude to my instructor Dr. Oleg Heczko for his persuading me to start with my doctoral studies and for his immense help, support, trust and patience from the very beginning of my studies till the very end. I thank him also for introducing the world of magnetism to me and for being a great colleague and my friend.

I would like to thank my supervisors of my major subject Prof. Toivo Katila and Prof. Ari Koskelainen and supervisors of my minor subject Prof. Veikko Lindroos and Prof. Simo-Pekka Hannula for giving me the opportunity to study in their laboratories and for their help and support during my studies. I am grateful to all people involved in the MSM-project for being a good team and nice colleagues, especially to Dr. Outi Söderberg, Dr. Yanling Ge, Dr. Andrés Ayuela, Dr. Jussi Enkovaara, Dr. Kari Ullakko, Nataliya Lanska M.Sc., Dr. Alexei Sozinov and Marjatta Aav M.Sc. I thank Dr. Yuriy Yagodzinskyy from Laboratory of Engineering Materials for his help and for his persuading me to continue and finish the work. I also thank Dr. Václav Novák from Institute of Physics ASCR and Dr. Michal Landa from Institute of Thermomechanics ASCR for interesting collaboration in the field of MSM alloys.

I acknowledge all the funding organizations: The National Technology Agency of Finland (Tekes), Outokumpu Research Oy, Adaptamat Oy, Nokia Research Center, Metso Paper Oy, ABB Corporate Research Oy, Foundation of Technology in Finland (TES), Helsinki University of Technology and Academy of Finland.

I thank all my friends, especially Jan Žižka and Hana Žižková M.Sc., for helping me to survive the dark Finnish winters. My very special thanks go to my parents, my brother Michal and his wife Alena, to my brother Jakub and his wife Hanka.

In Espoo, December 2006

Ladislav Straka

List of publications I–VII

I L. Straka, O. Heczko, V. Novák, and N. Lanska, **Study of Austenite-Martensite Transformation in Ni-Mn-Ga Magnetic Shape Memory Alloy**, Journal de Physique IV 112 (2003) 911–915.

II O. Heczko, L. Straka, N. Lanska, K. Ullakko, and J. Enkovaara, **Temperature Dependence of Magnetic Anisotropy in Ni-Mn-Ga Alloy Exhibiting Giant Field-induced Strain**, Journal of Applied Physics 91 (2002) 8228–8230.

III L. Straka and O. Heczko, **Investigation of Magnetic Anisotropy of Ni-Mn-Ga Seven-layered Orthorhombic Martensite**, Journal of Magnetism and Magnetic Materials 272–276 (2004) 2049–2050.

IV O. Heczko and L. Straka, **Temperature Dependence and Temperature Limits of Magnetic Shape Memory Effect**, Journal of Applied Physics 94 (2003) 7139–7143.

V L. Straka and O. Heczko, **Superelastic Response of Ni-Mn-Ga Martensite in Magnetic Fields and a Simple Model**, IEEE Transactions on Magnetics 39 (2003) 3402–3404.

VI L. Straka, O. Heczko, **Magnetization Changes in Ni-Mn-Ga Magnetic Shape Memory Single Crystal During Compressive Stress Reorientation**, Scripta Materialia 54 (2006) 1549–1552.

VII L. Straka, O. Heczko, S.–P. Hannula, **Temperature Dependence of Reversible Field-induced Strain in Ni-Mn-Ga Single Crystal**, Scripta Materialia 54 (2006) 1497–1500.

Author's contribution

The Author has contributed largely to design, development and maintenance of experimental apparatus for measurements of magnetic and magneto-mechanical properties, which have been used to carry out the experimental work presented in this Thesis. The Author has actively participated in planning of the experiments reported in the Publications and has been an initiator of the experimental investigations presented in Publications I, IV–VII. He has been responsible for carrying out all the experimental work related to measurements of magnetic properties and magneto-mechanical effects in the Publications. The Author has contributed substantially to evaluation and interpretation of experimental data and in a writing process of the Publications. He has had the main responsibility in writing of Publications I, III, V–VII. The Author has also contributed to another publications in the field of magnetic shape memory alloys, the list of which is included in References.

Short summary of the Publications

Publication I

The aim of publication *"Study of Austenite-Martensite Transformation in Ni-Mn-Ga Magnetic Shape Memory Alloy"* is to investigate the possibility of influencing martensitic transformation by external forces in such a way that a specimen consisting of a single martensitic variant is obtained after transformation. The study explores the effects of magnetic field up to 1 T and of compressive stress up to 4 MPa on the character of martensitic transformation and on the final martensite microstructure of a $Ni_{49.7}Mn_{29.1}Ga_{21.2}$ alloy. It is shown that application of 4 MPa compressive stress or of 1 T magnetic field during the transformation ascertain development of a nearly single martensitic variant in the specimen.

Publication II

Publication *"Temperature Dependence of Magnetic Anisotropy in Ni-Mn-Ga Alloy Exhibiting Giant Field-induced Strain"* focuses on investigation of magnetic anisotropy of $Ni_{48.8}Mn_{28.6}Ga_{22.6}$ alloy with a five-layered modulated tetragonal crystal structure. Dependence of the first anisotropy constant $K_{u1}(T)$ is determined from measured magnetization curves of a rectangular parallelepiped single crystal specimen in temperature range of 130–315 K; $K_{u1}(130\,\mathrm{K}) = 2.65 \times 10^5\,\mathrm{J \cdot m^{-3}}$, $K_{u1}(285\,\mathrm{K}) = 2.0 \times 10^5\,\mathrm{J \cdot m^{-3}}$. Measurement of the magnetization curves of a thin disc is also presented. It is shown that the second anisotropy constant is negligible and is not higher than 4% of K_{u1}. The publication also presents observation of a large magnetic shape memory effect by means of simultaneous measurement of strain and magnetization during the effect. This measurement corroborates the basic mechanism of the magnetic shape memory effect.

Publication III

Publication *"Investigation of Magnetic Anisotropy of Ni-Mn-Ga Seven-layered Orthorhombic Martensite"* focuses on investigation of magnetic anisotropy of a $Ni_{50.5}Mn_{29.4}Ga_{20.1}$ crystal with a seven-layered modulated orthorhombic crystal structure. A procedure used for obtaining the specimen containing a single martensitic variant, which is needed for correct determination of anisotropy constants, is presented in the publication. Magnetic anisotropy constants are determined from measured magnetization curves of the specimen in the temperature range allowed by the stability of the structure, i.e. 296–340 K. At room temperature, $K_1 = 1.7 \times 10^5\,\mathrm{J \cdot m^{-3}}$, $K_2 = 0.9 \times 10^5\,\mathrm{J \cdot m^{-3}}$, $K_3 \approx 0$.

Publication IV

In publication *"Temperature Dependence and Temperature Limits of Magnetic Shape Memory Effect",* the temperature dependence of magnetic shape memory effect

(MSME) is investigated on $Ni_{49.7}Mn_{29.1}Ga_{21.2}$ single crystal. A theoretical model of the MSME is employed for prediction of the temperature range in which the MSME can be observed. The measured temperature dependence of twinning stress in the range of 113–307 K shows a very steep increase at low temperatures. This implies that the MSME will be suppressed at low temperatures. The model calculation using measured twinning stress, magnetic anisotropy and tetragonal distortion of the lattice predicts that the MSME is suppressed below 165 K. This agrees rather well with direct measurement of the MSME, which gives the limit of $173(\pm 20)$ K. High temperature limit is imposed by start of reverse martensitic transformation at 315 K.

Publication V

Study *"Superelastic Response of Ni-Mn-Ga Martensite in Magnetic Fields and a Simple Model"* shows an alternative way of exploiting the magnetic shape memory effect. Instead of the typical configuration of the experiment with quasistatic magnetic field, the magnetic field is kept constant and $Ni_{49.7}Mn_{29.1}Ga_{21.2}$ single crystal is loaded by a compressive stress. The alloy behaves as a magnetic-field-controlled "superplastic" (for lower fields of 0–0.3 T) or "superelastic" material (for field $\geq$0.4 T). A reversible strain close to 6% is observed. The main features of magnetic-field controlled "superelastic" and "superplastic" behavior are modeled and compared with the experiments.

Publication VI

Study "*Magnetization Changes in Ni-Mn-Ga Magnetic Shape Memory Single Crystal During Compressive Stress Reorientation*" complements Publication V. It presents experimental observations of magnetization changes of $Ni_{48.5}Mn_{30.8}Ga_{20.7}$ specimen loaded compressively in static magnetic fields of up to 1.15 T. It is shown that the magnetization-strain dependency is monotonic, nonlinear and posses a small hysteresis. The maximum change of relative magnetization, about 30%, is observed at about half of the saturation field.

Publication VII

Publication "*Temperature Dependence of Reversible Field-induced Strain in Ni-Mn-Ga Single Crystal*" demonstrates that the shape changes associated with the magnetic shape memory effect can be made fully reversible when opposing stress is applied to a specimen with a very low twinning stress. The reversible strain observed on $Ni_{49.7}Mn_{29.1}Ga_{21.2}$ single crystal lies near the theoretical maximum, i.e. 6%, at room temperature but decreases considerably, to 1–2%, between 263 K and 253 K. The temperature and stress dependency of the observed reversible and maximum strains are interpreted using a theoretical model of the magnetic shape memory effect and comparison between the model and experiment is drawn. The condition of full reversibility of the magnetic shape memory effect is formulated.

Abbreviations and symbols

5M	five-layered modulated approximately tetragonal martensite with short c-axis
7M	seven-layered modulated approximately orthorhombic martensite
a-axis	crystallographic axis
b-axis	crystallographic axis
c-axis	crystallographic axis
AC	alternating current
DC	direct current
$L2_1$	order group, symmetry group
MSM	magnetic shape memory
MSME	magnetic shape memory effect
NM	tetragonal martensite with long c-axis
SQUID	superconducting quantum interference device
T	tetragonal martensite with long c-axis; Tesla (SI unit)
VCM	vibrating coil magnetometer
VSM	vibrating sample magnetometer
A_f	transformation temperature (finish of reverse martensitic transformation)
A_s	transformation temperature (start of reverse martensitic transformation)
a_A, a_M	lattice parameter of austenite, lattice parameter of martensite
b_A, b_M	lattice parameter of austenite, lattice parameter of martensite
c_A, c_M	lattice parameter of austenite, lattice parameter of martensite
H	magnetic field strength
H_A, H_{A1}, H_{A2}	anisotropy fields
l	length of a specimen
l_0	initial length of a specimen
K_1, K_2, K_3	magnetocrystalline anisotropy constants
M	magnetization
M_{001}	magnetization along [001] axis
M_{100}	magnetization along [100] axis
M_S	saturation magnetization
M_s	transformation temperature (start of martensitic transformation)
M_f	transformation temperature (finish of martensitic transformation)
T_C	Curie temperature
x, y, z	Cartesian coordinates
$\alpha_1, \alpha_2, \alpha_3$	direction cosines
ε	experimental (macroscopic) strain
ε_0	distortion of the lattice

ε_{MAX}	maximum strain
ε_r	reversible strain
φ	polar coordinate
χ	volume fraction of induced martensitic variant
μ_0	permeability of vacuum (air), $\mu_0 = 4\pi \times 10^{-7}\,\mathrm{H{\cdot}m^{-1}}$
σ_{EXT}	external stress
σ_{TW}	twinning stress
σ_M	magnetic stress
θ	polar coordinate

Contents

1 Introduction

1.1 Magnetic shape memory alloys

The magnetic shape memory (MSM) alloys present a new class of materials, which are receiving considerable interest from scientific groups and industry. They are similar to shape memory alloys (SMAs), with which they share many common properties. They, in fact, form a special subclass of SMAs. The essential requirement for a material to belong to the group of shape memory alloys is that the thermoelastic martensitic transformation occurs in it, during which the higher-symmetry parental phase transforms to lower-symmetry daughter phase, called martensite [1]. The typical way of inducing this transformation is cooling the material below the martensitic transformation temperature (M_S). A reverse transformation can be observed when the material is heated from temperature below M_s to a higher temperature denoted usually as A_S ($M_s < A_\mathrm{S}$). The product of martensitic transformation, martensite, is a mesoscopic structure (microstructure), the arrangement of which is reflected in macroscopic shape of the material. The martensite microstructure can be manipulated by mechanical stress, which leads to large macroscopic strains of up to several percent or even larger in some cases. This effect is usually denoted as superplasticity. The martensitic and reverse transformation can be further accompanied by shape changes. This is usually called shape memory effect (SME). The material can reconstruct its original shape during reverse transformation (one-way SME), restoring from previous shape changes induced by manipulation of martensite microstructure. It can even switch between two defined shapes by undergoing martensitic and reverse transformations (two-way SME). Other unusual mechanical properties of SMAs include superelasticity, rubberlike behavior etc. [1].

What makes the magnetic shape memory alloys distinct from ordinary shape memory alloys and what makes them quite unique among any material is that the martensite microstructure can be manipulated by exposing them to a magnetic field, Figure 1. This can lead to large macroscopic strains of several percent induced only by the magnetic field. Additionally, these changes can be "remembered" by the martensite microstructure. The first observation of this kind of rearrangement on Ni-Mn-Ga was made by Ullakko *et al.* in 1996 [2]. They demonstrated 0.2% strain in stoichiometric $Ni_{50}Mn_{25}Ga_{25}$[1] specimen induced by 0.8 T magnetic field and they interpreted the effect as result of rearrangement of martensite microstructure. Strains of 4–6% of Ni-Mn-Ga alloys caused by a magnetic field close to 1 T were demonstrated by various groups in 1999–2000, see e.g. Refs. [3–6]. The largest magnetic-field induced shape change in Ni-Mn-Ga MSM alloy so far observed, with strain almost 10%, was presented by Sozinov *et al.* in 2002 [7] and Müllner *et al.* in 2004 [8]. The history and development of the Ni-Mn-Ga MSM alloys are well described in Refs. [9, 10]. The shape changes due to rearrangement of martensite microstructure in a magnetic

[1] The $Ni_xMn_yGa_z$ labeling of the alloys is used throughout this work, where x is atomic % of Ni, y is atomic % of Mn, z is atomic % of Ga in the alloy, $x+y+z=100$.

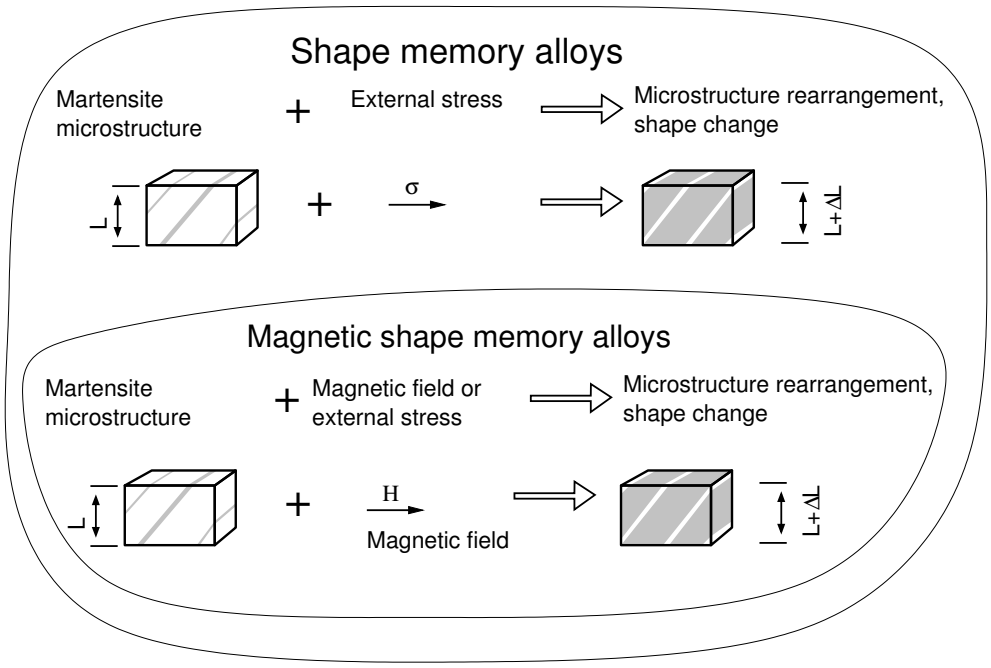

Figure 1: Shape memory alloys and their relation to magnetic shape memory alloys.

field have been also observed in Ni-Mn-Ga-Fe [11], Fe-Pd [12], and La-Sr-CuO_4 [13] alloys. The antiferromagnetic order in La-Sr-CuO_4 and a suggestion of antiferromagnetic order in Ni-Mn-Ga [14] justify the term "magnetic shape memory alloys" as more appropriate than a relatively often used term "ferromagnetic shape memory alloys", see, e.g., Refs. [6, 15, 16].

It is worth noting here that behavior of terbium and dysprosium in magnetic field is very similar to the behavior of MSM alloys. About 4–7% magnetic-field-induced strain due to formation of mechanical twins (plastic deformation) was observed on terbium and dysprosium single crystals in large magnetic fields (10–40 T) as soon as in 1965 and 1975 [17] (pages 275–276), [18].

Thus, in MSM alloys, the interactions between the magnetic field and the martensite microstructure lead to shape changes induced by the magnetic field. The changes of the martensite microstructure are, on the contrary, reflected in macroscopic magnetic behavior of the material. For example, the net macroscopic magnetization and magnetization curve of the alloy change when the magnetic martensite microstructure is rearranged by mechanical stress [19, 20], [Publication VI]. The term magnetic shape memory effect (MSME) is used throughout this work for interactions between magnetic field and martensite microstructure resulting in shape changes.

Generally, the shape changes induced by magnetic field are denoted as magnetostriction. Due to similarity of behavior of MSM alloys and the well known magnetostrictive materials (e.g. Terfenol) it is tempting to equal the terms MSME and magnetostriction. But the necessity of existence of martensite microstructure and its

active role in shape changes and especially its "memory" make the MSME very different from ordinary magnetostriction. Thus, distinction of the MSME, which is essentially a mesoscopic effect, from ordinary magnetostriction, which is an atomic-level microscopic effect, must be made. Using the theoretical apparatus developed for ordinary magnetostriction is neither justifiable nor can it predict the highly extraordinary magnetomechanical interactions observed in MSM alloys. More detailed discussion of differences between ordinary magnetostriction and MSME is given in Ref. [15].

A common argument justifying scientific research, development and utilization of the MSM alloys is that the alloys combine the best properties of the SMAs and ordinary magnetostrictive materials. They are potentially able to actuate at large strains (up to 10%) and large frequencies (at least 1 kHz) with nearly a perfect efficiency of coupling of magnetic energy to mechanical load [15,21–25]. Promising possibilities of embedding sensing, actuation and even control into the structure of the material itself, or, in other words, using it as an "intelligent" material [26] are also considered [9]. Consequently, the MSM alloys are not just a better shape memory or "magnetostrictive" material but their complex behavior due to the MSME can possibly be utilized in totally new applications.

Present work focuses exclusively on Ni-Mn-Ga magnetic shape memory alloys because of the availability of this material and its very good performance of MSME. Apart from MSME, the Ni-Mn-Ga MSM alloys exhibit several other interesting properties [27], e.g. conventional shape memory effect, traditional superelasticity, magnetocaloric and special transport properties (large magnetoresistance [28]) and large elastic anisotropy [29].

1.2 Objectives of the research

A broad research effort targeting the Ni-Mn-Ga MSM alloys was carried out at Helsinki University of Technology in the framework of the Magnetic Shape Memory Project (MSM-project) during 1998–2003. The aims of the MSM-project included modelling, materials processing, characterization and research of magnetic properties of the MSM alloys in close cooperation with industrial partners. Present work is based mainly on the results obtained by the Author in MSM-project during 2000–2003. At the time when the work on the Thesis started, the properties of the Ni-Mn-Ga alloys were mostly unknown. The MSME was a very new phenomenon and only few research groups worldwide reported observation of this effect. The true mechanism of MSME was still being discussed at the time (a detailed discussion continues up to this date) and only few models of the effect were available.

A general objective of any material research and development is to obtain material with the best properties for a given application. The most important property of the MSM alloys is the MSME, thus, the conditions of the existence of MSME are investigated in the presented work. The knowledge essential for engineering use of any material is the material's performance at high and low temperatures. Therefore, investigation of temperature dependence of the MSME, modelling of the dependence, and exploration of the temperature limits of the MSME were selected as some of the main aims of this work. As the MSME was a new phenomenon, the work also aimed to demonstrate, investigate, interpret and model the interplay between martensite microstructure and its magnetic properties and associated extraordinary magneto-mechanical effects as reversible MSME, magnetic-field induced superelasticity and changes of magnetization with changes of martensite microstructure. The objectives can be summarized in the following list:

- Developing the experimental apparatus suitable for investigation of MSM alloys and MSME.
- Exploring the possibilities of creating single variant specimens by different methods.
- Determining the magnetic and other material properties controlling the existence of MSME and their temperature dependences using single variant specimens.
- Experimental investigation and modeling of the effect of temperature on MSME.
- Experimental investigation and demonstration of the interplay of the martensite microstructure, its magnetic properties and magnetic field.
- Experimental investigation and demonstration of extraordinary magneto-mechanical effects in Ni-Mn-Ga alloys, i.e reversible MSME, magnetic-field controlled superelasticity, and changes of magnetization with changes of martensite microstructure (reorientation of martensite).

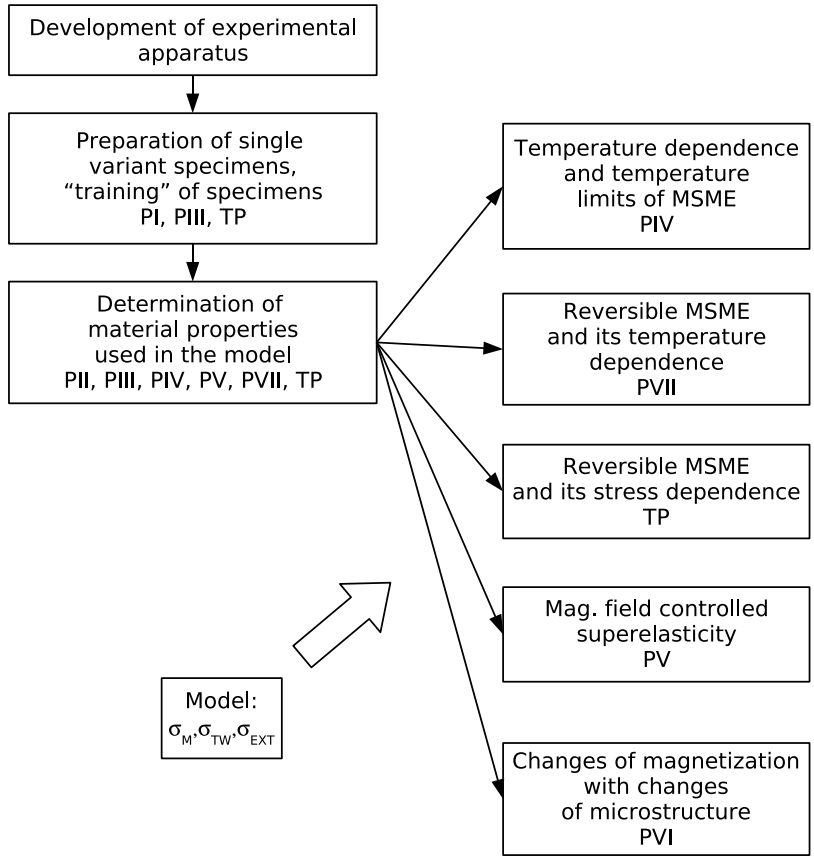

Figure 2: Structure of the work. Publications associated with the particular parts are indicated as follows: TP = this publication, PI = Publication I, PII = Publication II, etc.

1.2.1 Organization of the work

The structure of the work is shown in Figure 2. An essential part of the work was development of experimental apparatus used for investigation of MSME.

Presence of magnetic martensite microstructure in an MSM alloy is a necessity but not the only condition for existence of the MSME. Additionally, the martensitic variants constituting the microstructure must be properly oriented and arranged. Moreover, controlling the martensite microstructure is essential for magnetic and other studies. Acquiring a technique of creating a controlled arrangement of martensitic variants is, therefore, a basic requirement for any systematic investigation and utilization of MSME. That is why several possibilities of creating controlled configuration of the martensite microstructure (i.e., creating single variant specimen) were studied in Publication I and Publication III.

It follows from the model first proposed by Ullakko and Likchachev in 1999 [30] that there are three key material parameters controlling the existence of the MSME — magnetic anisotropy of the martensite, twinning stress (macroscopic parameter re-

flecting resistance of martensite microstructure to rearrangement), and distortion of the lattice. The work, therefore, focused intensively on experimental studies of these material parameters, these studies are presented in Publication II–Publication V and in Publication VII.

The experimentally determined parameters served as a basis for interpretation and modelling of the behavior of MSM alloys in various conditions, as shown in Figure 2. The most interesting phenomena studied were the temperature dependence of MSME (Publication IV) and of reversible MSME (Publication VII), influence of external stress on the existence and reversibility of MSME (Publ. VII), magnetic-field controlled superelasticity (Publication V), and changes of magnetization with rearrangement of martensite microstructure, i.e. with reorientation of martensite (Publication VI). The issue of "training" of the martensite microstructure, i.e. decreasing the twinning stress, was partly explored in this work.

The summary part of this Thesis gives short introduction about MSM alloys and objectives of the research (Chapter 1), necessary minimum general information about the Ni-Mn-Ga alloys and used theoretical model (Chapter 2) and describes used experimental methods and apparatus (Chapter 3). The most interesting properties of Ni-Mn-Ga alloys determined during the course of this work are summarized in Chapter 4, which presents selected original results some of which are new and complement the results given in the Publications.

2 Ni-Mn-Ga alloys

This chapter gives general introduction to the material properties of Ni-Mn-Ga alloys intended to support understanding of the results presented in this Thesis by a general reader. Crystal structure of Ni-Mn-Ga, observed types of martensite, mobility of twin boundaries, and used theoretical model of MSME are described.

2.1 Crystal structure of Ni-Mn-Ga alloys

A stoichiometric $Ni_{50}Mn_{25}Ga_{25}$ alloy has cubic, Heusler type ($L2_1$), crystal structure with lattice parameter $a = 0.5825\,\text{nm}$ at room temperature. This structure undergoes martensitic transformation at about 200 K and the product of this transformation has been identified by X-ray diffraction as modulated tetragonal martensite with lattice parameters $a = b = 0.5925\,\text{nm}$ and $c = 0.5563\,\text{nm}$ [31]. High resolution neutron diffraction indicates, however, that the structure is only approximately tetragonal, and, in fact, it is slightly orthorhombic or even monoclinic [32]. The large strains associated with the martensitic transformation are accommodated by twinning, i.e. by the formation of martensitic twin variants (martensitic variants, variants) and twin boundaries between them so that the internal energy is minimized. The different martensitic twin variants have the same primitive cell but different structural orientation [1].

The very low transformation temperature of the stoichiometric $Ni_{50}Mn_{25}Ga_{25}$ can be shifted above ambient temperature by slight adjustments of the alloy composition. The type of crystal structure, lattice parameters and magnetic properties also depend on the alloy composition. The transformation and crystallographic properties are usually mapped to average number of valence electrons per atom as presented e.g. in Refs. [33, 34]. The three observed martensite structures in a Ni-Mn-Ga bulk close to stoichiometric composition are usually marked as 5M (or 10M), 7M (or 14M) and T (or NM). They are described e.g. in Refs. [9, 33, 35, 36].

5M martensite The lattice of 5M, or five-layered modulated, martensite has an approximately tetragonal unit cell but is modulated by a five-layer periodic shuffling along $(110)[1\bar{1}0]_p$ system [37]. The tetragonal symmetry axes of the 5M are approximately parallel to the $\langle 100 \rangle$ directions of the parental cubic cell [30, 33]. The approximately tetragonal cell has ratio $c/a < 1$. There are three possible martensitic twin variants twinned on $\{110\}$ planes [30]. An excellent description of twins and martensitic variants in 5M is given in Ref. [38]. Most of the observations of MSME have been done for this type of martensite, including present study, and many others. 5M martensite is often termed the most promising candidate for practical applications.

7M martensite The 7M, or seven-layered modulated, martensite has an approximately orthorhombic structure with $c/a < 1$ modulated by a seven-layer periodic shuffling along $(110)[1\bar{1}0]_p$ system [37]. There are six possible martensitic twin variants

twinned on $\{110\}$ planes [8]. Only two observations of the MSME in this type of martensite have been published so far, with strain close to 10% [7, 8]. This Thesis presents experimental observation of a strain of about 4% due to MSME in this structure.

T martensite The T martensite has a tetragonal unit cell with $c/a > 1$. This martensite does not exhibit shape changes in magnetic field. Nevertheless, its mechanical behavior can be slightly influenced by magnetic field [39]. Possible deformation of this structure is about 20% [40]. For more details on T martensite, see Ref. [9].

2.2 Mobility of twin boundaries and twinning stress

The easiness of motion of the twin boundaries between martensitic variants of Ni-Mn-Ga alloys is striking and has been known for long [2] but it has not been satisfactorily explained. The modulation of the lattice may play some role in the extraordinary mobility of the twin boundaries, as the mobility in a non-modulated T martensite is an order of magnitude lower than in modulated 7M and 5M martensites. Application of 1–2 MPa external compressive stress along the $[100]$ direction of 5M or 7M martensite is sufficient for radical rearrangement of martensite microstructure by the motion of the twin boundaries [3, 37], while for T martensite at least 6–12 MPa stress is needed [7, 9, 37, 40]. The external stress inducing the rearrangement of martensite microstructure is usually denoted as twinning stress, σ_{TW} or $\sigma_{\mathrm{TW}}(\varepsilon)$, where ε is macroscopic strain caused by the rearrangement.

2.3 Model of magnetic shape memory effect

There are various models describing the magnetic shape memory effect in Ni-Mn-Ga in magnetic field. A short review on this topic can be found in Ref. [41]. In this work, a simplified version of model presented by Likhachev and Ullakko in 2000 [3] was used for several reasons. Firstly, this model was developed at the site of research, therefore, many aspects of this model could be discussed directly with its authors. Moreover, it was only one of a few models available at the time when the work on this Thesis started. The model is reasonably simple and its few material parameters can be easily determined by experiment. The model carries no arbitrary parameters. Thus, it has a considerable predictive potential as presented e.g. in Refs. [7, 30] and also in this Thesis. The essential assumption of the model is that the driving force for the twin boundary motion (i.e. rearrangement of the martensite microstructure) is the difference in magnetization free energies between different martensitic variants. From this follows immediately that the magnetic anisotropy of the alloy is a crucial parameter and that the driving force cannot exceed its saturation value. In a typical arrangement of the experiment used throughout this work, the magnetic driving force, σ_{M}, or "magnetic stress" is

$$\sigma_{\mathrm{M}}(H) = \frac{\int_0^H M_{001}(H)\mathrm{d}H - \int_0^H M_{100}(H)\mathrm{d}H}{\varepsilon_0} \tag{1}$$

where H is the strength of the magnetic field, $M_{001}$and M_{100} are magnetizations of the martensitic variants with [001] and [100] directions along the magnetic field and $\varepsilon_0 = 1 - c/a$ is the distortion of the lattice. When also the external stress, σ_{EXT}, is considered the model gives a net driving stress $\sigma_{\mathrm{M}}(H) - \sigma_{\mathrm{EXT}}$ [42]. The twin boundaries move as far as the condition

$$\sigma_{\mathrm{M}}(H) - \sigma_{\mathrm{EXT}} > \sigma_{\mathrm{TW}}(\varepsilon) \tag{2}$$

keeps satisfied. Based on this relation a macroscopic strain dependency $\varepsilon(H)$ can be easily determined. The $\sigma_{\mathrm{TW}}(\varepsilon)$ dependence and magnetization curves as well as the distortion of the lattice can be obtained experimentally.

In a simplified version of the model, $\sigma_{\mathrm{TW}}(\varepsilon)$ dependency is replaced by a single value, which corresponds to the position of the plateau on the stress strain curve. This is justifiable for specimens with a very flat plateau. The maximum possible driving force can be determined from Equation 1 as

$$\sigma_M^{max} = K_1/\varepsilon_0 \tag{3}$$

where K_1 is uniaxial anisotropy constant of the martensite. Using this simplification, the existence of MSME can be predicted using the relation

$$\frac{K_1}{\varepsilon_0} > \sigma_{\mathrm{TW}} + \sigma_{\mathrm{EXT}}. \tag{4}$$

When this relationship is satisfied, large MSME with strains close to distortion of the lattice will be observed in large enough field. Alternatively, one can choose any arbitrary macroscopic strain $\varepsilon < \varepsilon_0$ and use the condition

$$\frac{K_1}{\varepsilon_0} > \sigma_{\mathrm{TW}}(\varepsilon) + \sigma_{\mathrm{EXT}} \tag{5}$$

for prediction of a possibility of observing this "threshold" macroscopic strain.

Thus, according to the model, there are three key material parameters controlling the existence of the MSME — magnetic anisotropy of the martensite, twinning stress, and distortion of the lattice. Knowledge of these three material parameters is sufficient for prediction of the existence of MSME.

3 Experimental methods

In this chapter, apparatus used for experimental investigation are described alongside with used experimental methods and contribution of Author to the apparatus development. Developed apparatus for AC susceptibility measurement, vibrating sample magnetometer and MSM-apparatus are described. The key factors determining selection of the composition of the studied alloys are explained in the end of this chapter.

3.1 Apparatus for AC susceptibility measurement

The AC susceptibility measurement was used for the following: determination of the Curie points of Ni-Mn-Ga specimens, determination of temperatures of martensitic and reverse transformations, and detection of intermartensitic transformations. It was demonstrated e.g. in Ref. [43] that the changes of AC susceptibility correspond well to transformation temperatures of a Ni-Mn-Ga alloy determined by differential scanning calorimetry measurements.

The AC susceptibility measurement is based on the change of mutual inductance of a primary coil and two identical but oppositely wound secondary coils with the specimen placed in one of them. The primary coil (long solenoid) is coaxial with the two secondary coils positioned inside it. The same type of arrangement is presented e.g. in Ref. [44]. A flow of nitrogen gas is used for cooling, an auxiliary coil (bifilary-wound) is used to heat the specimen. Temperature of the specimen is measured by a thermocouple. A lock-in amplifier is used to generate the driving signal (488Hz) and to measure the signal from secondary coils, which is proportional to the (complex) AC susceptibility of the specimen. The data are logged and the measurement is controlled by a personal computer using the IEEE488 interface.

The Author's contribution to the development of this apparatus comprised of the design and implementation of temperature control of the device. He also rewrote from scratch the main control program of the device. This allowed to set time dependency of temperature prior to the measurement by means of filling a table containing temperature limits and heating and cooling rates. The improvements of the apparatus made by the Author enabled convenient automatic measurement of AC susceptibility in a wide temperature range.

3.2 Vibrating sample magnetometer

The vibrating sample magnetometry is one of the most common methods for measurement of magnetization [45, 46]. It was first introduced by Foner in 1959 [47]. It is an induction technique, which detects the AC magnetic field produced by an oscillating magnetic moment. A magnetized specimen oscillates at a low frequency (20 Hz) and induces signal proportional to magnetization in pick-up coils. The measurements of magnetization and magnetization curves is one of the most useful tools for investigation of magnetic materials, hence for MSM alloys. Magnetic anisotropy and satura-

tion magnetization are determined exploiting the magnetization curves. The shape of the magnetization curve reveals information about the existence of MSME and about distribution of martensitic variants. Additionally, measurement of DC susceptibility combined with the measurement of magnetization curves reveals information about structure transformations [48].

The Author has contributed largely in design and building of the vibrating sample magnetometer. He redesigned the main vibrating mechanism and associated mechanical parts, participated in design of cryostat, designed and built a polarity current switch and implemented software for temperature control and software controlling the measurement. The improvements made by the Author allowed unattended sophisticated measurements of magnetization curves at various temperatures and also measurement of DC susceptibility and saturation magnetization as functions of temperature. The improvements also increased reliability, stability and sensitivity of the magnetometer, which on its turn allowed using the magnetometer even for measurement of Ni-Mn-Ga thin films [49].

3.3 MSM-apparatus

For the purposes of the MSM-project, a device for measurement of mechanical properties comprising of a cylinder and a piston driven by a compressed air was constructed. A specimen is enclosed between two copper parts, which transmit the force from the piston to the specimen. Heating of the specimen is done by means of electrical heating of these copper parts. Cooling of the specimen below room temperature is facilitated by introducing a stream of cold nitrogen gas into the specimen region.

The above described device was combined with a vibrating coil magnetometer[2]. This combination resulted in unique instrument which allows for a simultaneous measurement of strain and magnetization as functions of external stress, magnetic field and temperature. This instrument is termed *MSM-apparatus* in following text. The mechanical part of the MSM-apparatus is shown schematically in Figure 3.

The Author's contribution to this apparatus was design and implementation of temperature control executed by software and design and implementation of a complex software which allowed various kinds of measurement via control of the magnetic field, temperature, or stress as well as simultaneous monitoring of stress, strain, and magnetization. The Author implemented a laser interferometer into the apparatus, allowing a well calibrated measurement of large strains. The Author also participated largely in multiple improvements and continuous maintenance of this apparatus during the course of the research.

[2]The vibrating coil magnetometer works on similar principles as the vibrating sample magnetometer but the pick-up coils vibrate instead of the sample [50]. This arrangement allows to carry out magnetization measurements for such specimen which cannot be vibrated for some reason.

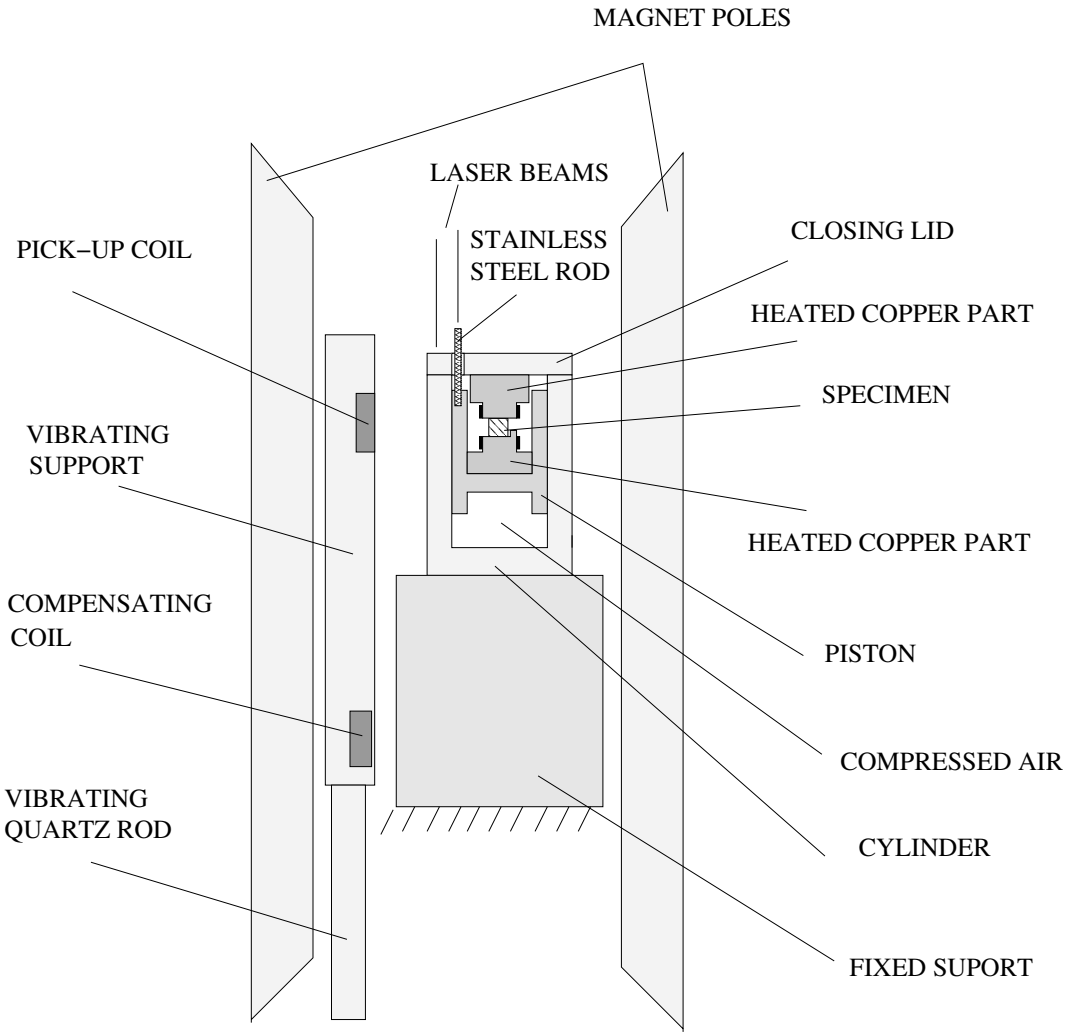

Figure 3: Schematic drawing of the MSM-apparatus designed for measurement of magneto-mechanical properties of MSM alloys. The specimen is loaded by a piston driven by compressed air. The position of the piston copies the dimension of the specimen and is tracked by laser interferometer. Vibrating coil magnetometer uses two coils – a pick-up coil and a coil compensating for voltage induced due to the presence of a large field of the magnet.

Typical experimental arrangement The identical experimental arrangement was used for studying the magneto-mechanical properties of MSM alloys throughout this work, consequently all results refer to this type of arrangement unless otherwise said. Single crystal specimens had typically form of a rectangular parallelepiped with the faces along $\{100\}$ set planes of the cubic cell of $L2_1$ or along $\{100\}$ and $\{001\}$ set planes of the tetragonal cell (for 5M martensite) or along $\{100\},\{010\},\{001\}$ set of planes of the orthorhombic cell (for 7M martensite). The typical size of specimen was $4\,\mathrm{mm} \times 5\,\mathrm{mm} \times 9\,\mathrm{mm}$. Magnetic field and stress were always applied perpendicularly

to each other along two of the three principal axis of the specimen and strain was measured along the direction of the stress. Several modes of measurement were used:

- Stress and temperature were kept constant and magnetic field was increased and decreased quasistatically. Strain and magnetization were obtained as functions of magnetic field. This mode was used for observation of MSME in quasistatic magnetic field.
- Magnetic field was zero, temperature constant and stress was increased and decreased. Strain was obtained as a function of stress. In such a way, twinning stress was determined. This mode also served for training of martensite microstructure.
- Magnetic field was nonzero and constant, temperature constant, and stress was increased and decreased. Strain and magnetization were obtained as functions of stress. This mode of measurement was used for investigation of magnetic-field controlled superelasticity and for study of changes of magnetization with changes of martensite microstructure (reorientation of martensite).
- Stress was constant, magnetic field constant and temperature was changed at a constant rate. Strain and magnetization were monitored. This mode mostly served for studies of martensitic transformation but also for direct observation of low temperature limit of MSME.

Further description of experimental methods is given in the Publications and partly in Chapter 4.1.

3.4 X-ray diffraction, EDS, and optical microscopy

The X-ray diffraction studies were mostly done by N. Lanska using Philips X'pert single crystal X-ray diffractometer. Composition of the alloys was determined using energy dispersive spectroscopy (EDS) by Y. Ge or by Outokumpu Research Center Oy, Finland. Presented optical microscopy studies were performed by the Author. Using polarized light enabled to observe martensite bands even on completely flat surfaces due to different optical activity of martensitic variants with different orientations.

3.5 Selection of composition

Although experiments made by Author served as supportive information in development, selection and production of new Ni-Mn-Ga alloys, Author was not directly involved in this process. To date, there is no established criterion for the alloy selection and the selection of the optimal composition remains one of the problem of the research of Ni-Mn-Ga alloys. Since, the selection and production of Ni-Mn-Ga alloys is not described in this Thesis.

The main criterion for the selection of the alloys and specimens for investigation was any performance of MSME, i.e., alloy or a specimen was usually selected for investigation if it was a good candidate for existence of MSME. The good candidates were rather scarce, and, additionally, the studied specimens got often destroyed during the experiments due to their brittleness. Therefore, due to the scarcity of specimens, the composition was minor parameter for selection of the specimens, the main parameter was MSME performance and that is why the composition of the alloys varies in Publications and in summary part of this Thesis. Sometimes the composition was changed because a new (better) alloy was developed and knowledge of its properties was important for the research group. The varying composition is not considered crucial for this work since many of the presented results have general character describing general behavior of Ni-Mn-Ga MSM alloys (or 5M or 7M martensites) rather than behavior of only one particular composition.

4 Results

4.1 Martensitic transformation in Ni-Mn-Ga alloys

In this chapter, aspects of martensitic transformation important for this Thesis are presented. Changes of strain and magnetization associated with martensitic transformation are described and possibility of creating single variant specimen is discussed. Magnetization curves of single variant specimen are presented.

4.1.1 Strain associated with martensitic transformation

Martensitic transformation from $L2_1$ cubic parental phase to 5M martensite is illustrated in Figure 4a. The transformation temperatures for $Ni_{48.6}Mn_{26.3}Ga_{25.1}$, an example of a typical MSM alloy, as determined from AC susceptibility curve are $A_s \approx A_f = 317\,\mathrm{K}$ and $M_s \approx M_f = 308\,\mathrm{K}$ [Publication I]. The very narrow hysteresis (9 K) between the transformation temperatures indicates that the martensitic transformation is thermoelastic, i.e. the interface between the parent phase and the martensite is highly mobile and the driving force for martensitic transformation is small [1].

There are three possible martensitic variants in the 5M martensite with the three principal axes of the tetragonal lattice unit lying approximately along the three principal axes of the cubic structure. These variants form a twinned microstructure and are separated from each other by twin boundaries. Distribution of the martensitic variants in a specimen is generally arbitrary after the martensitic transformation. Some information about the variant distribution after the martensitic transformation can be obtained by dilatation measurement as illustrated in Figure 4b, which also shows the experimental arrangement. The strain caused by the transformation is measured along one edge of a specimen in form of rectangular parallelepiped (with faces along the $\{100\}$ set of planes of the cubic phase). The principal axes of all the three tetragonal martensitic variants (the $[001], [010], [100]$ directions) are approximately parallel to the principal axis of the parental cubic phase. Therefore, when the whole volume of the specimen transforms to martensitic variant with the short axis (i.e. $[001]$ direction) along the measured edge, the strain of $(c_\mathrm{M} - a_\mathrm{A})/a_\mathrm{A} = -3.92\%$ should be observed. When, on the contrary, this variant is not present at all after the transformation, the observed magnitude of strain should be $(a_\mathrm{M} - a_\mathrm{A})/a_\mathrm{A} = 1.82\%$. However, when this is the case, there can still be two variants present in the specimen, with different orientations of the short axis (perpendicular to the measured strain). Any strain inside these margins indicates that there is a mixture of two or three variants in the specimen. Note that the lattice parameters were not determined exactly at the transformation temperature but at room temperature (approx. 297 K) and at 323 K. Thus, the real margins of strain can slightly differ from the predicted limits since there is a large change of lattice parameters close to the transformation [51].

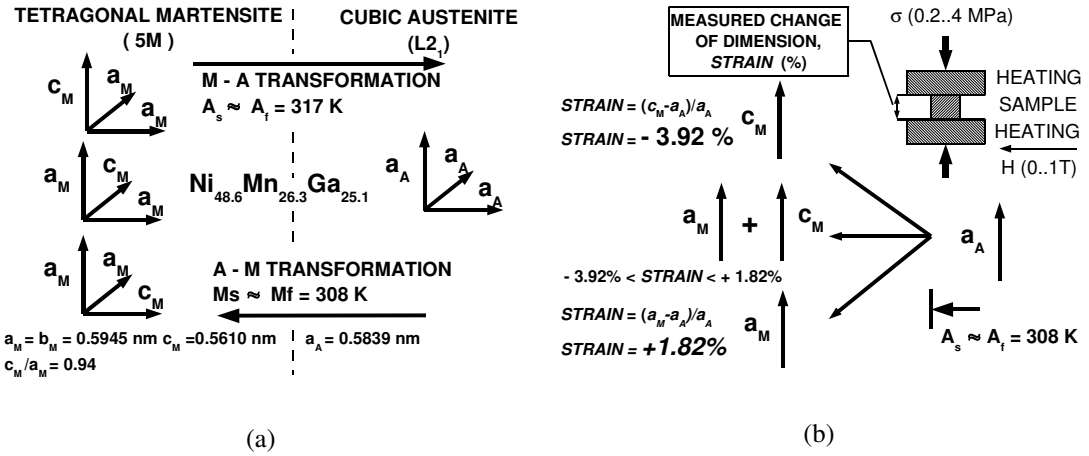

(a) (b)

Figure 4: Martensitic transformation in $Ni_{48.6}Mn_{26.3}Ga_{25.1}$ alloy and the effect of variants arrangement on observed macroscopic strain. a) Changes of crystal structure during martensitic and reverse transformation. The presented lattice parameters were determined at room temperature (approx. 297 K) for martensite and at 323 K for austenite. b) Possible observed strain during martensitic transformation for different final distribution of martensitic variants (different microstructure) in indicated experimental arrangement.

4.1.2 Changes of magnetization during martensitic transformation

The parental phase is magnetically soft, $K_1(295\,\mathrm{K}) = 2.7 \times 10^4 \mathrm{ergs/cm^3}$ ($= 2.7 \times 10^3\,\mathrm{J/m^3}$) [52], while the 5M martensite exhibit large uniaxial magnetic anisotropy ($K_1(283\,\mathrm{K}) = 2.0 \times 10^5 \mathrm{J/m^3}$ [Publication II]) with easy axis of magnetization (easy axis[3]) along $[001]$. Consequently, the arrangement of variants (i.e. martensite microstructure) and progress of the martensitic transformation reflect in changes of AC and DC susceptibility of the specimen. Measurement of strain and DC susceptibility during martensitic and reverse transformation is shown in Figure 5. Figure 5a shows the case where most of the volume of the specimen transforms to a tetragonal martensitic variant with the $[001]$ direction along the measured strain, which is deduced from magnitude of strain of -3.4%. The DC susceptibility is measured perpendicularly to the strain along $[100]$ direction of the parental phase. The tetragonal martensitic variant with $[001]$ direction along the strain has $[100]$ direction (hard axis), along the direction of DC susceptibility measurement. Thus, a decrease of DC susceptibility is observed during the martensitic transformation as this variant forms and, vice versa, the DC susceptibility increases during reverse transformation where this variant is replaced by

[3]The $[100]$ direction will be referred to as *hard axis* since it is difficult to magnetize the martensite along it, Figure 8. Note that the $[100]$ and $[010]$ directions are equivalent in the tetragonal crystal structure of 5M martensite; they form, in fact, (001) *hard plane.*

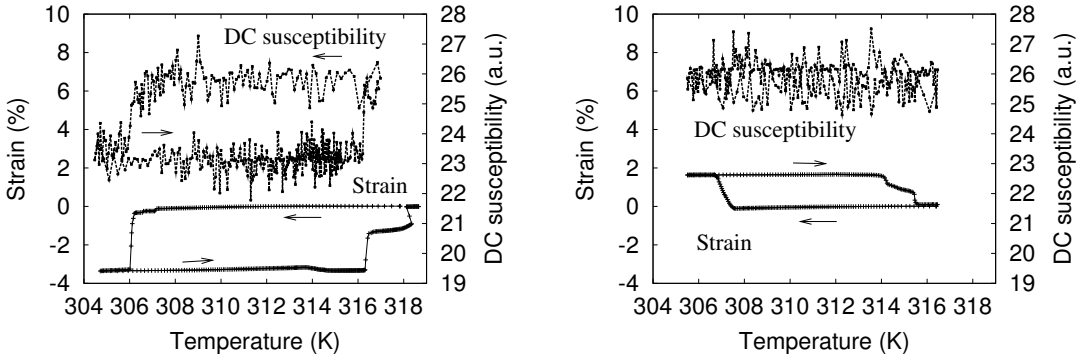

Figure 5: Observation of strain and DC susceptibility measured by MSM-apparatus (Chapter 3.3) during martensitic and reverse transformation of $Ni_{48.6}Mn_{26.3}Ga_{25.1}$ alloy. The DC susceptibility was measured perpendicularly to the measured strain in magnetic field of approximately 0.005 T. Cooling/heating rate was 1–2 K/min. The large noise observed on DC susceptibility curve is caused by a relatively low sensitivity of the vibrating coil magnetometer.

the magnetically soft parental phase. Figure 5b shows a situation where 1.8% strain caused by martensitic transformation is observed. This magnitude of strain indicates that the specimen constitutes of variants with [100] direction along strain measurement direction. Since the DC susceptibility shows almost no change, it can be deduced that most of the volume of the specimen consists of a variant with [100] direction along the strain measurement and [001] (easy axis) along the DC susceptibility measurement. Similar considerations apply for AC susceptibility measurements, which are much more sensitive [62].

Martensitic transformation can also be detected by a measurement of saturation magnetization, since the parental phase exhibits lower saturation magnetization than the martensitic phase [52]. This phenomenon was investigated in Ref. [48]. It was shown that it can be used for monitoring the progress of martensitic transformation in situations where dilatation measurement cannot be used directly as, e.g., in thin films [53]. The saturation magnetization as a function of temperature during cooling is shown in Figure 6a. As the Curie temperature is relatively close to the martensitic transformation temperatures, the saturation magnetization increases rapidly with decreasing temperature. The martensitic transformation is observed as a sudden increase of saturation magnetization, which is indicated by an arrow in Figure 6a. The saturation magnetization does not depend on the arrangement of martensitic variants (martensite microstructure). Simultaneous measurement of strain and saturation magnetization in 1 T field during martensitic and reverse transformation is shown in 6b. The changes of structure are clearly reflected in the changes of saturation magnetization.

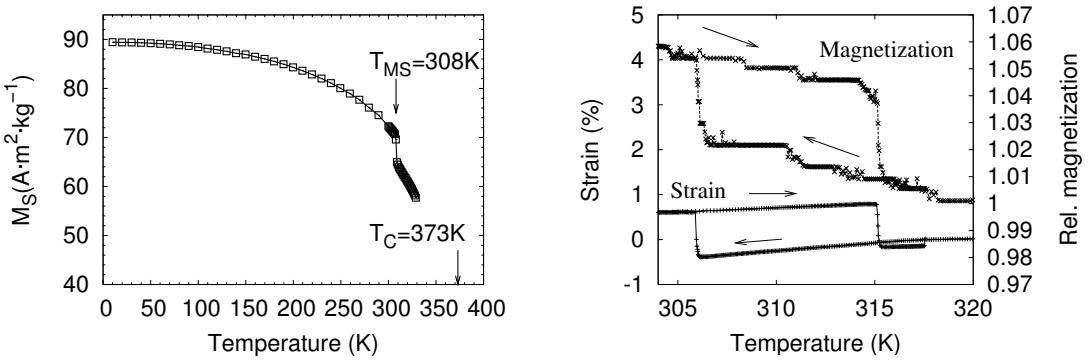

(a) (b)

Figure 6: Saturation magnetization along the [100] direction of parental phase of $Ni_{48.6}Mn_{26.3}Ga_{25.1}$ alloy. a) Measured by SQUID magnetometer during cooling in a 2 T field with cooling rate 6 K/min. Since the saturation magnetization of the martensite is higher than the saturation magnetization of parental structure, the martensitic transformation can be detected on the curve. Courtesy of Oleg Heczko. b) Simultaneous measurement of strain and relative magnetization in a 1 T field during martensitic and reverse transformation with cooling/heating rate 1–2 K/min. Measured by MSM-apparatus described in Chapter 3.3. The small steps observed on the magnetization curve are caused by a relatively low resolution of the apparatus, large changes of magnetization (about 4%) in coincidence with strain changes are caused by martensitic transformation.

4.1.3 Single variant specimen production

For investigation of magnetic and other properties of MSM alloys and for obtaining the largest shape changes due to the MSME, it is preferable to have single variant specimens, i.e. specimens containing only single martensitic variant. This can be facilitated by applying additional force during the martensitic transformation, i.e external stress or magnetic field. The applied stress makes the growth of the variant with a short axis ([001] direction) along the stress energetically more favourable, while the magnetic field makes the growth of the variant with a short axis ([001] direction, easy axis) along the field energetically more favourable. An example of such effect for various magnitudes of compressive stress (0.2–4 MPa) and magnetic field (0, 0.5, 1 T) is shown in Figure 7. Without the external forces the transformation behavior is rather random. When a medium stress (1–4 MPa) or magnetic field (1 T) is applied, it facilitates the creation of the single variant specimen. This is deduced from measured strain and magnetization.

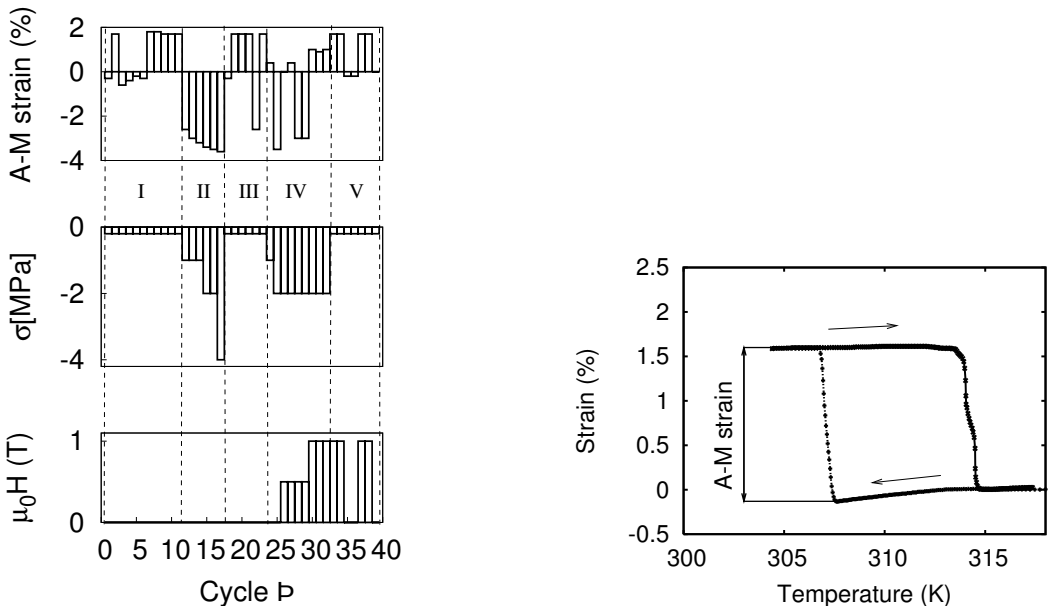

(a) (b)

Figure 7: a) Effect of external stress and magnetic field on strain associated with martensitic transformation of $Ni_{48.6}Mn_{26.3}Ga_{25.1}$ MSM alloy. The data are taken from the Publication I (Table 1), where details of measurement can be found. In total, 39 transformation cycles (austenite-martensite-austenite) were measured with various magnitudes of compressive stress and magnetic field. The total strain obtained during each transformation from austenite to martensite (A-M strain) was evaluated from the monitored strain. Magnitudes of the applied stress, applied magnetic field and determined A-M strain for each cycle are given in three separate bar charts. The five regions marked in the charts correspond to: I: Cycles 1–11 — nearly zero external forces. II: Cycles 12–17 — large compressive stress. III: Cycles 18–23 — nearly zero external forces. IV: Cycles 24–32 — certain combinations of stress and field. V: Cycles 33–38 — nearly zero stress, large or zero field. b) Determination of A-M strain from monitored strain.

4.1.4 Magnetization curves of single variant specimen

Magnetization curves of single variant specimen measured along the [100] and [001] directions are shown in Figure 8. The structure exhibit uniaxial magnetic anisotropy with easy axis along [001] direction. The very small hysteresis of the curve measured along the [100] direction indicates that the magnetization process along this hard axis is mainly due to magnetization rotation. The magnetization curve of $L2_1$ parental cubic structure measured along the [100] direction is shown for comparison in the same figure.

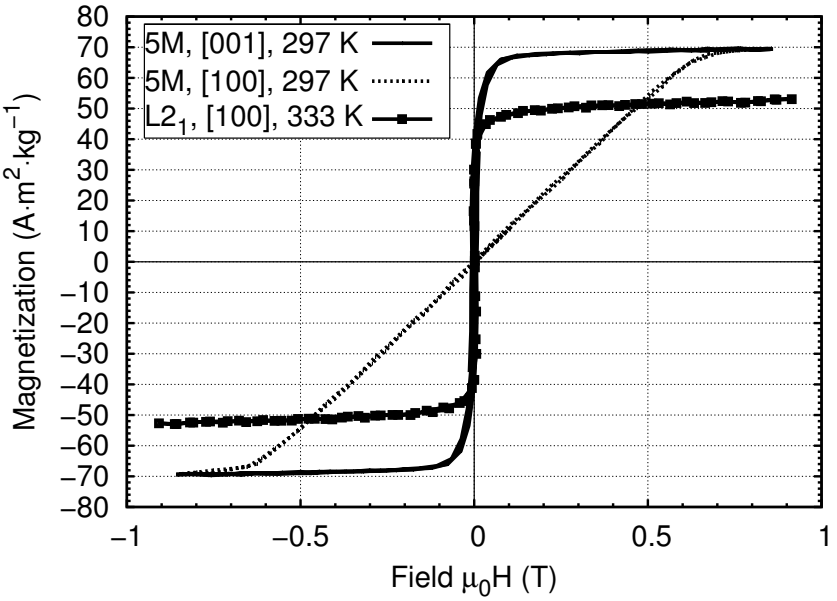

Figure 8: Magnetization curves of $Ni_{48.6}Mn_{26.3}Ga_{25.1}$ alloy. The specimen (rectangular parallelepiped) was compressed by approximately 10 MPa stress during measurement along the [100] direction of 5M martensite to prevent MSME. The curves were corrected for demagnetization.

4.1.5 Conclusion

The martensitic transformation in 5M martensite is accompanied by large (nearly 4%) shape changes and by large changes of DC and AC susceptibility as well as saturation magnetization (about 4%). The changes occur due to crystal transformation from cubic to tetragonal. The changes of strain, susceptibility and magnetization provide information about progress of the transformation and arrangement of martensitic variants (martensite microstructure). Application of a medium stress (1–4 MPa) or magnetic field (1 T) during martensitic transformation facilitates the creation of a single variant specimen. Determined magnetization curves of such a specimen shows that the structure has uniaxial anisotropy with easy axis along [001] direction.

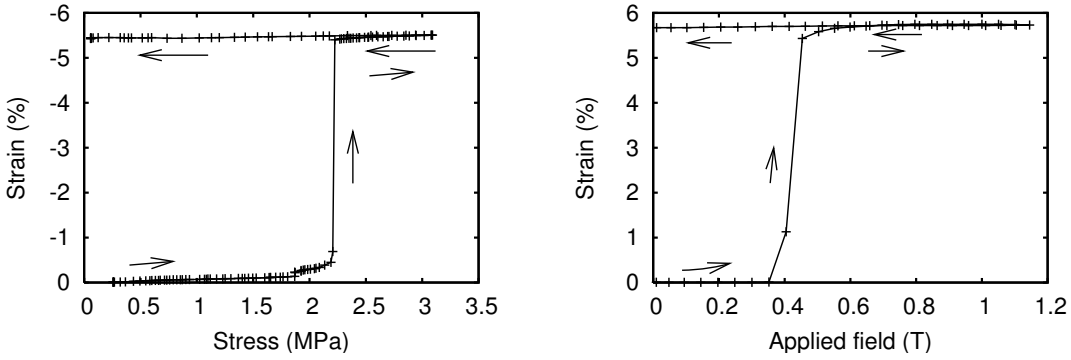

(a) (b)

Figure 9: Manipulation of martensite microstructure of $Ni_{48.6}Mn_{26.3}Ga_{25.1}$ MSM alloy. a) Using external compressive stress — a single variant specimen with the [100] direction along the external stress (created by martensitic transformation in 1 T magnetic field) is reoriented by the external stress in such a way that it has the [001] direction along the external stress after the experiment. Contraction of the specimen along the external stress is observed. b) Using quasistatic magnetic field and nearly zero external stress — the single variant specimen with the [100] direction along the magnetic field (created by compression as shown on the left) is reoriented by the magnetic field in such a way that it has the [001] direction along the magnetic field after the experiment. Contraction of the specimen along the magnetic field and elongation along the external stress are observed. This is the magnetic shape memory effect. Note that the strain is measured along the external stress, perpendicularly to the applied field.

4.2 Magnetic shape memory effect

This chapter describes the most interesting property of the Ni-Mn-Ga alloys, the MSME. Reorientation of martensite (rearrangement of martensite microstructure) accompanied by straining of alloy and changes of magnetization during the MSME are explained as well as their interrelation.

4.2.1 Shape changes induced by an external stress and by magnetic field

Martensite microstructure of magnetic shape memory alloys can be manipulated either by external stress or by magnetic field. In a typical experimental arrangement (Chapter 3.3), a very low compressive external stress of about 2.2 MPa is enough to reorient a $Ni_{48.6}Mn_{26.3}Ga_{25.1}$ single variant specimen. The specimen having initially the [100] direction along the external stress has the [001] direction (short axis) along the external stress after the compression. This $[100] \Rightarrow [001]$ reorientation along the stress is accompanied by -5.4% strain, Figure 9a. Simultaneously with the $[100] \Rightarrow [001]$ reorientation along the stress, $[001] \Rightarrow [100]$ reorientation along the magnetic field oc-

Table 1: Ideal reorientation of martensite in two subsequent steps. Initially, the three principal axes x, y, z coincide with the three principal axes ([100], [010], [001] directions, respectively) of the tetragonal cell of the structure. Compression is performed along the x-axis ([100] direction), which reorients the martensite. After the compression, the x-axis coincides with the [001] direction, the z-axis coincides with the [100] direction. Magnetic field applied along the z-axis ([100] direction) of the reoriented martensite produces the initial orientation. The theoretical strains along the principal axes associated with the reorientations are given in the table (strain x =strain along the x-axis, etc.).

	x	y	z	strain x	strain y	strain z
Initial	[100]	[010]	[001]	-	-	-
Compression along x	[001]	[010]	[100]	-5.63%	0	5.97%
Magnetic field along z	[100]	[010]	[001]	5.97%	0	-5.63

curs. In a subsequent experiment, Figure 9b, a relatively small magnetic field of about 0.5 T restores the original shape of the specimen. It causes $[100] \Rightarrow [001]$ reorientation along the magnetic field accompanied by simultaneous $[001] \Rightarrow [100]$ reorientation along the stress. A strain of 5.7% is observed in direction of stress, perpendicular to the field. The observed large shape change due to magnetic field is the *magnetic shape memory effect* or MSME.

Maximum possible theoretical strain for complete reorientation of the martensite is $(c_M - a_M)/a_M = -5.63\%$ along $[100] \Rightarrow [001]$ reorientation and it is $(a_M - c_M)/c_M = +5.97\%$ along $[001] \Rightarrow [100]$ reorientation (lattice parameters are given in Figure 4a). These strains are correlated, i.e. as the specimen elongates in one direction, it contracts in one of the other two perpendicular directions while its volume remains constant. The strain is zero along the third direction. These shape changes can be expressed by strain tensor as e.g. in Refs. [3, 41]. An ideal case of the reorientation of the $Ni_{48.6}Mn_{26.3}Ga_{25.1}$ single variant specimen is described in Table 1. The magnitudes of strains observed in Figure 9 (i.e. -5.4% and 5.7%) are very close to the ideal strains ("strain x" in Table 1) which confirms that the specimen was single martensitic variant before and after the reorientations and that the reorientations were complete. The specimen consists of two martensitic variants during the reorientation with one of the variants growing at the expense of the other one. The growth of the variant is facilitated by motion of the twin boundaries between the martensitic variants, i.e. rearrangement of martensite microstructure. Observation of this process by optical microscopy is shown in Figure 10.

4.2.2 Changes of magnetization during MSME

As said earlier, 5M martensite has the easy axis of magnetization (easy axis) along the [001] direction, while the [100] direction is hard axis (Figure 8). It is, therefore,

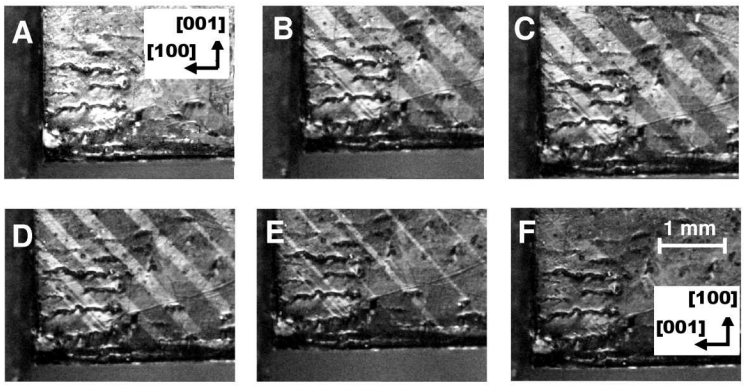

Figure 10: Development of surface morphology of a $Ni_{48.6}Mn_{26.3}Ga_{25.1}$ rectangular parallelepiped specimen during reorientation of martensite by compression. Crystallographic orientations of the initial (A) and final (F) martensitic variants are indicated. Using optical microscopy with polarized light it was observed that the new variant grows with increasing stress as 45 degrees inclined dark bands (lamellae) in an original variant (B–E). After magnetic field was applied instead of stress, so that the observed strain was about 3%, similar pattern as in C was obtained.

possible to monitor the reorientation of the martensite in quasistatic magnetic field (Figure 9b) by measurement of magnetization, which is shown in Figure 11b. For a small field, the magnetization curve follows the curve of the hard axis (Figure 11a), and only magnetization rotation occurs away from the easy axis perpendicular to the field. As the field increases, the martensite starts reorienting at a certain magnitude of the field, which can be observed as a sudden increase on the magnetization curve. After the reorientation is complete, the curve follows the curve measured for the easy axis (Figure 11c). This leads to a hysteresis in the first quadrant of the magnetization curve, Figure 11b. This hysteresis is typical sign of MSME [54]. The martensite remains in the reoriented state, which can be deduced from a measurement of strain, Figure 9b, i.e. a subsequent application of magnetic field in the opposite direction has no effect on the martensite and no hysteresis is observed on the magnetization curve in the third quadrant. The same applies for subsequent magnetization cycles, Figure 11c — no hysteresis is observed and no shape changes occur. To obtain the MSME repeatedly, martensite must be reoriented after application of magnetic field, e.g. by compression, by rotating the specimen, by rotating the field, etc.

4.2.3 Interrelation between martensite microstructure and magnetization

A simultaneous measurement of strain and magnetization in an experiment with quasistatic magnetic field is shown in Figure 12. The observed simultaneous changes of strain and magnetization demonstrate the interrelation between the martensite microstructure, shape, and magnetization of a MSM alloy. Additionally, the measurement

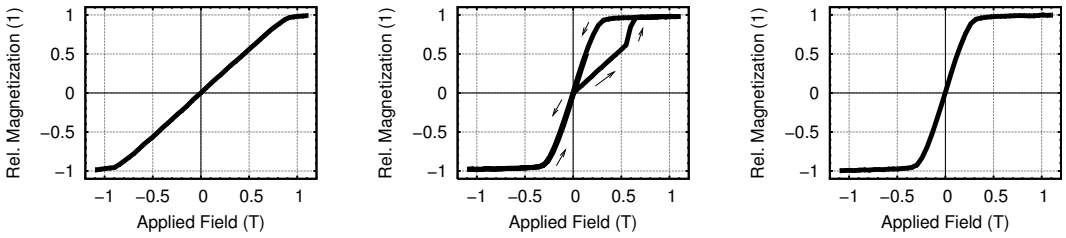

(a) (b) (c)

Figure 11: Typical magnetization curves of an alloy exhibiting the MSME ($Ni_{48.6}Mn_{26.3}Ga_{25.1}$). a) The specimen after martensitic transformation under external compressive stress of 8 MPa. Magnetization curve is measured under the same stress to prevent MSME. b) Measurement subsequent to the measurement shown in (a) — for the same specimen exposed to external stress of 0.2 MPa MSME occurs. This is observed on the magnetization curve as the first quadrant hysteresis. c) Measurement subsequent to the measurement shown in (b) — martensite is already reoriented and no MSME occurs. The curves were not corrected for demagnetization. Corrected curves along [100] and [001] directions are shown in Figure 8.

corroborates that the mechanism of MSME is due to a twin boundary motion (i.e., rearrangement of martensite microstructure) as proposed originally by Ullakko *et al*. [2].

4.2.4 Conclusion

Full reorientation of martensite with strain close to 6% can be achieved either by applying external stress of about 2 MPa or magnetic field of about 0.4 T. The mechanism of the rearrangement was confirmed by optical microscopy and also by simultaneous measurement of strain and magnetization to be due to motion of twin boundaries. The (irreversible) MSME is indicated on the magnetization curves as the first quadrant hysteresis.

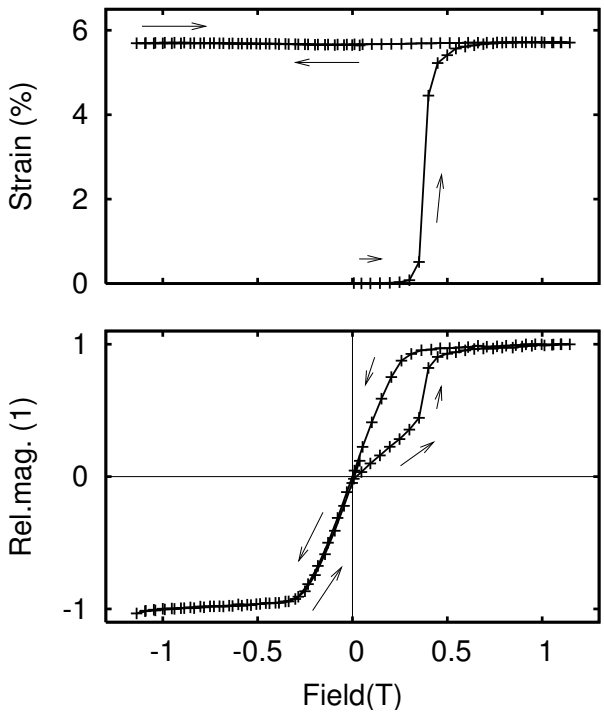

Figure 12: Simultaneous measurement of strain and magnetization of $Ni_{48.6}Mn_{26.3}Ga_{25.1}$ single variant specimen (5M martensite) in a typical experiment with a quasistatic magnetic field. The first quadrant hysteresis on magnetization curve presents a typical sign of the occurrence of MSME. Since no MSME occurs for negative field (martensite is already reoriented due to magnetization in positive field), there are neither any large strain changes observed for negative field, nor is there large hysteresis observed on magnetization curve in the third quadrant.

4.3 Key parameters determining the existence of MSME

In this chapter, material parameters essential for existence of MSME and their temperature dependencies are discussed. Using of the experimentally determined temperature dependencies in the theoretical model for determining the temperature limits of the MSME is demonstrated.

4.3.1 Key parameters

As already discussed in Chapter 2.3, the model by Likhachev and Ullakko used in this Thesis assumes that the driving force for the MSME is the difference in the magnetization free energies between the martensitic variants. The model predicts the existence of MSME when one of the Relationships 2–5 (Chapter 2.3) is satisfied. From the relationships it follows that large magnetic anisotropy, small twinning stress and small distortion of the lattice are the most important parameters determining the existence of

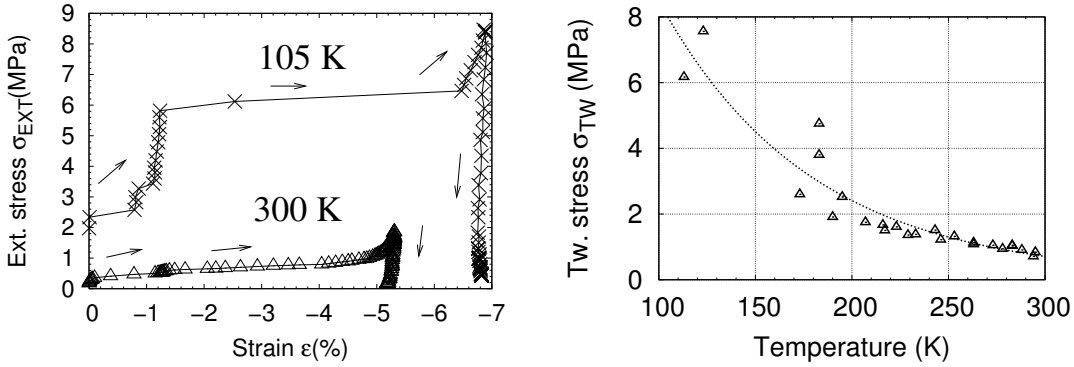

(a) (b)

Figure 13: Twinning stress in $Ni_{48.6}Mn_{26.3}Ga_{25.1}$ alloy (5M martensite). a) Measurement of stress-strain curve during $[100] \Rightarrow [001]$ reorientation along external compressive stress at 300 K and 105 K. Twinning stress is determined as the external stress necessary to obtain -3% strain in this experiment. This stress corresponds well to the position of plateau on the stress-strain curve. b) Temperature dependence of the twinning stress with the dashed curve serving as guide for the eyes.

MSME in a MSM alloy. These parameters depend on many factors, the most important of which are probably the composition of the alloy and the temperature [9, 55]. Additionally, the twinning stress may depend on homogeneity of the alloy, obstacles and impurities present in the alloy, as well as on the thermo-mechanical-magnetic history of the alloy. The latest will be shown below.

4.3.2 Distortion of the lattice

Distortion of the lattice, $\varepsilon_0 = 1 - c/a$, is increasing with decreasing temperature; $\varepsilon_0(300\text{K}) \approx 5.5\%$, $\varepsilon_0(4\text{K}) \approx 7.5\%$ for a 5M martensite [56]. From the model used in this Thesis it follows, that a larger driving force is necessary to achieve MSME in an alloy with a larger distortion of the lattice. Thus, the increase of the distortion of the lattice with decreasing temperature is hindering the possibility of MSME.

Finding an alloy with distortion of the lattice smaller than usual, e.g. 1%, could allow MSME even for higher twinning stress or external stress (assuming the same magnetic properties). On the contrary, large distortions, about 10% in a 7M martensite or 20% in a T martensite, are hindering the MSME. This is one of the reasons why MSME is difficult to observe in a 7M martensite [7] or is not observed in a T martensite at all [39].

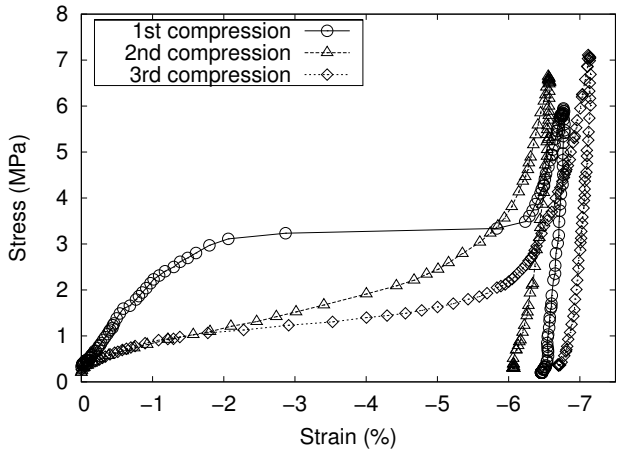

Figure 14: Twinning stress development of a $Ni_{49.7}Mn_{29.1}Ga_{21.2}$ specimen after martensitic transformation under 7 MPa compressive stress. The specimen was compressed repeatedly along two edges. The chart presents a measurement along one of the edges. The twinning stress decreases rapidly for the first three compressions and remains approximately the same for the fourth and fifth compressions as it was for the third one (not shown in the chart for the sake of clarity).

4.3.3 Twinning stress

Twinning stress is determined from the position of the plateau on the stress-strain curve of a specimen compressed along the $[100]$ direction. The twinning stress increases with decreasing temperature, which was shown e.g. in Refs. [39, 55] and in Publication IV. The increase can be rather significant. Measurement of the twinning stress in $Ni_{48.6}Mn_{26.3}Ga_{25.1}$ alloy is shown in Figure 13. The twinning stress increases from about 1 MPa at room temperature to about 8 MPa at 105 K. Additionally, the stress-strain curves, Figure 13a, reveal that the distortion of the lattice changes with decreasing temperature as the total strain due to $[100] \Rightarrow [001]$ reorientation increases from -5% at 300 K to nearly -7% at 105 K. Although the twinning stress initially grows linearly with decreasing temperature, the growth becomes more steep, exponential-like, for low temperatures far from martensitic transformation. The large increase of the twinning stress is the main limiting factor for the existence of MSME in this particular alloy.

Twinning stress depends on thermo-mechanical-magnetic history of the martensite. This is demonstrated in Figure 14. The twinning stress is much larger in a specimen immediately after martensitic transformation than the twinning stress measured after repeated compressions of the specimen along two edges. After a few compressions, the twinning stress remains approximately constant. The effect was not studied in a detail but a possible explanation is that there may have been a small amount of interlocked martensitic variants of various orientation in the specimen, which block the reorientation of martensite. With repeated compression, these variants disappear

gradually. Additionally, the specimen could be a very pure single variant before the first compression and the nucleation of the other variants during the first compression needed larger energy than a simple motion of the twin boundaries of the existing bands or embryos of the other variant during the following compressions.

Compression is not the only way to change the twinning stress. Similar effect can be achieved by rotating the specimen in 1 T magnetic field. In such a way a considerable amount of specimens originally not exhibiting any MSME was made to display the MSME, i.e. the twinning stress must have been lowered by the rotation.

An example of a twinning stress reduction by mechanical training finalized by treatment of the specimen in magnetic field for a 7M martensite is shown in Figure 15. By repeated compression of the specimen along two edges and by rotation in 1 T magnetic field the twinning stress can be reduced significantly and MSME is observed, Figure 15d. The reorientation due to the MSME is only partial, however. This is inferred from the magnitude of the strain being only 4.2% instead of close to $\varepsilon_0 \approx 10\%$, which would be the expected magnitude for a full reorientation of this type of a martensite. The small magnitude of strain can be explained according the model using the Relationship 2 (Chapter 2.3). It is assumed that the martensite reorients directly from the variant with the long axis ([100] direction) along the field to the variant with short axis ([001] direction) along the field (the variant distribution after reorientation was not checked). Anisotropy constant of the $Ni_{50.5}Mn_{29.4}Ga_{20.1}$ alloy is determined in Publication III as $K_1 = 1.7 \times 10^5\,\mathrm{J \cdot m^{-3}}$. Consequently, the maximum available magnetic stress is $\sigma_M = K_1/\varepsilon_0 = 1.7 \times 10^5/0.1 = 1.7\,\mathrm{MPa}$. External stress 0.2 MPa is used for fixation of the specimen during the measurement, i.e. $\sigma_M - \sigma_{EXT} = 1.5\,\mathrm{MPa}$. This value of stress corresponds to 4.6% strain on the stress-strain curve (Figure 15, curve 8) and it is the maximum strain expected to be obtained due to magnetic field. The observed maximum value of the strain is 4.2%, Figure 15d, showing that the agreement with the model is good. Similar considerations and results were presented in Ref. [7] by Sozinov *et al.* with the exception that they observed larger strain, 9.5%, in 1.05 T magnetic field. The decrease of twinning stress with mechanical training in the 7M martensite is also presented in Ref. [57]. Treatment of a 7M martensite by rotating magnetic field is shown in Ref. [8] where an initial 6% strain increased to almost 10% strain after 140 rotations of a specimen in magnetic field of about 1 T.

So far, no satisfactory model describing the twinning stress has been developed. Some authors propose using statistical approach for modelling the twinning stress [58, 59]. The statistical approach is, however, hard to accept for specimens studied in this work, in which only several (1–10) bands (lamellaes) of a martensitic variant are observed, see e.g. Figure 10 and Figure 2 in Publication IV.

4.3.4 Magnetic anisotropy

Probably the first investigation of magnetic anisotropy of the Ni-Mn-Ga alloy showing the MSME was presented in Ref. [52]. Magnetic anisotropy is also mentioned in various other works on Ni-Mn-Ga as e.g. in Refs. [3, 60]. Compositional and temperature

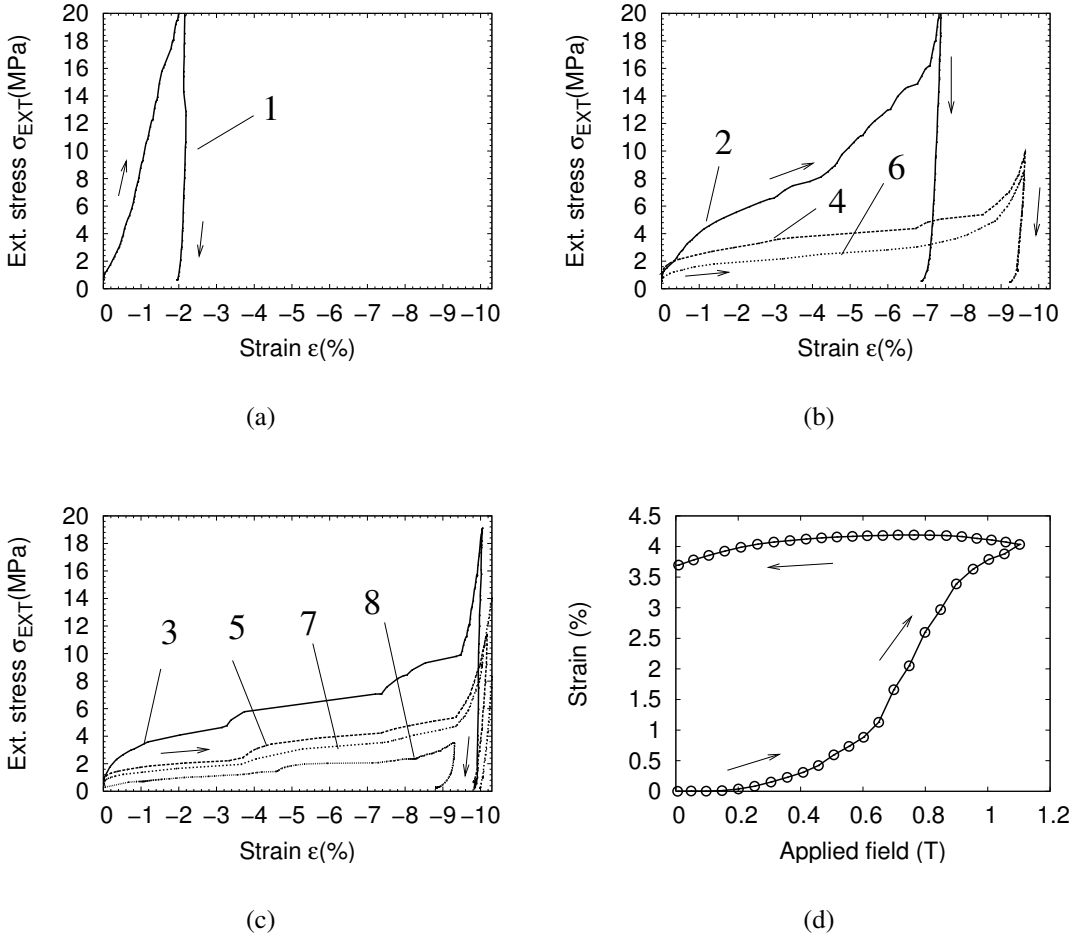

Figure 15: Reduction of twinning stress of a 7M martensite ($Ni_{50.5}Mn_{29.4}Ga_{20.1}$) by mechanical and magnetic treatment. Radical decrease of twinning stress is observed. Subfigures (a), (b), (c) represent measurements of stress-strain curves along three edges of the specimen. The specimen was first compressed along one edge (a) and then repeatedly along the other two edges (b), (c) in a sequence indicated by numbers. After the 7th cycle the specimen was additionally rotated several times in 1 T magnetic field, which led to a further decrease of twinning stress, (c), cycle 8. The obtained very low value of twinning stress allowed observation of MSME in a 7M martensite (d), however, with only part of the martensite reoriented by magnetic field. Subfigure (d) with courtesy of Oleg Heczko.

dependence of magnetic anisotropy of polycrystalline Ni-Mn-Ga alloys was studied by Albertini *et al*. [61]. Nevertheless, most observations of MSME are obtained in single crystal specimens. The effect of temperature on magnetic properties and magnetic anisotropy of a single crystal exhibiting MSME was also mentioned in Ref. [62]. A study of dependence of magnetic anisotropy on the composition for a 5M martensite

was presented in Ref. [63]. Dependence of magnetic anisotropy on martensite type is discussed in Refs. [37, 64].

In the present work, the temperature dependencies of magnetic anisotropy of a 5M and a 7M martensites were studied using single-crystal single-variant specimens (Publication II and Publication III). These reports show that magnetic anisotropy of Ni-Mn-Ga MSM alloys increases with decreasing temperature. The increase of the anisotropy compensates partly for increasing distortion of the lattice and twinning stress. Thus, it extends the possibility of MSME to lower temperatures (Relationship 4 in Chapter 2.3).

Determination of magnetic anisotropy of single crystals with known symmetry can be made based on a measurement of magnetization curves of a single crystal along relevant crystallographic directions and calculation of the differences in magnetization energy [65, 66]. In an ideal case, a thin disc (cut in such a way that the disc plane contains the directions of interest) is measured. Using a thin disc suppresses the shape effects, i.e. reduces the demagnetization field and corner effects. Production of thin discs for the measurements was successful only partially since manipulation of the martensite microstructure in a thin disc often resulted in a fracture of the disc. The manipulation had to be done to create a single variant specimen, which is necessary for obtaining of magnetization curves along the selected directions.

It was necessary to constrain the disc against mechanical rotation and to prevent MSME during measurement of magnetization curves. However, the surface relief caused by shape changes associated with the manipulation of the martensite microstructure made the faces of the disc non-flat. As a result, it was impossible to constrain the disc properly. Polishing of the faces to remove the surface relief produced undesired variants in the martensite microstructure again. Additionally, the fracture of the disc often occurred in magnetic field.

A small number of discs was produced and measured. Due to the above mentioned problems, however, specimens in a form of a rectangular parallelepiped were used for most of the measurements. This requires corrections of the magnetization curves for shape effects and many unwanted corner effects, but still, it extends considerably the possibilities of manipulation and constrain of the martensite microstructure and makes the measurement of magnetization curves reliable. The rectangular parallelepiped can be compressed along three directions and can easily be constrained against rotation in magnetic field by fixing at its side (the rotation occurs due to magnetic anisotropy of the specimen). The correction of the magnetization curves for demagnetization was made by means of measurement of magnetization curves of a Ni specimen of the same dimensions and evaluation of the demagnetization factor based on these curves. In a limited number of cases measured specimens were heated through reverse transformation and magnetization curves of austenite (magnetically very soft, Chapter 4.1) were measured and used to determine the demagnetization factor.

Anisotropy constants The potential magnetization energy per unit volume for tetragonal crystal is [65]

$$E = K_1 \sin^2\theta + K_2 \sin^4\theta + K_3 \sin^4\theta \cos 4\varphi + \ldots, \tag{6}$$

where θ, φ are polar coordinates and K_1, K_2, K_3 are the first, second and the third anisotropy constants. For orthorhombic crystal [65]

$$E = K_1\alpha_1^2 + K_2\alpha_2^2 + K_3\alpha_3^2 + K_4\alpha_1^2\alpha_2^2 + K_5\alpha_1^4 + \ldots \tag{7}$$

where $K_1, K_2, K_3, \ldots$ are anisotropy constants and $\alpha_1, \alpha_2, \alpha_3$ are direction cosines.

The magnetization curves of the 5M (Figure 8) and 7M martensites (Publication III) are perfectly linear and show small hysteresis. This means that only the anisotropy constants of lowest order are important (i.e. K_1 for 5M martensite and K_1, K_2, K_3 for 7M martensite) and that the magnetization process is dominated by rotation of magnetization [65]. In such a case, the conception of anisotropy field (H_A) can be used to determine magnetic anisotropy [65]. Then, for 5M martensite (uniaxial crystal with preferred c-axis) it applies

$$K_1 = \frac{1}{2} M_S H_A, \tag{8}$$

where M_S is saturation magnetization and H_A is anisotropy field. For 7M martensite (orthorhombic crystal with preferred $c-$axis, i.e. $K_3 = 0$) it applies

$$K_1 = \frac{1}{2} M_S H_{A1}, \tag{9}$$

$$K_2 = \frac{1}{2} M_S H_{A2}, \tag{10}$$

where M_S is saturation magnetization and H_{A1}, H_{A2} are anisotropy fields in pertinent directions.

The anisotropy field can be determined as the position of a knee on magnetization curve measured in a relevant direction. We have determined this position as the intersection between linear extension of the initial part of the magnetization curve and saturation magnetization. This allows estimation of magnetic anisotropy even in situations when MSME and associated large (first-quadrant) hysteresis on the magnetization curve are observed. Alternatively, the anisotropy constants can be determined from the area between magnetization curves measured in relevant directions [65, 66], but this does not allow estimation of anisotropy in situations with MSME. Chernenko *et al*. have recently pointed out that the relation between anisotropy field and distortion of the lattice is proportional with changing temperature [67]. It may, thus, allow determination of temperature dependence of tetragonal distortion from temperature dependence of anisotropy field and vice versa.

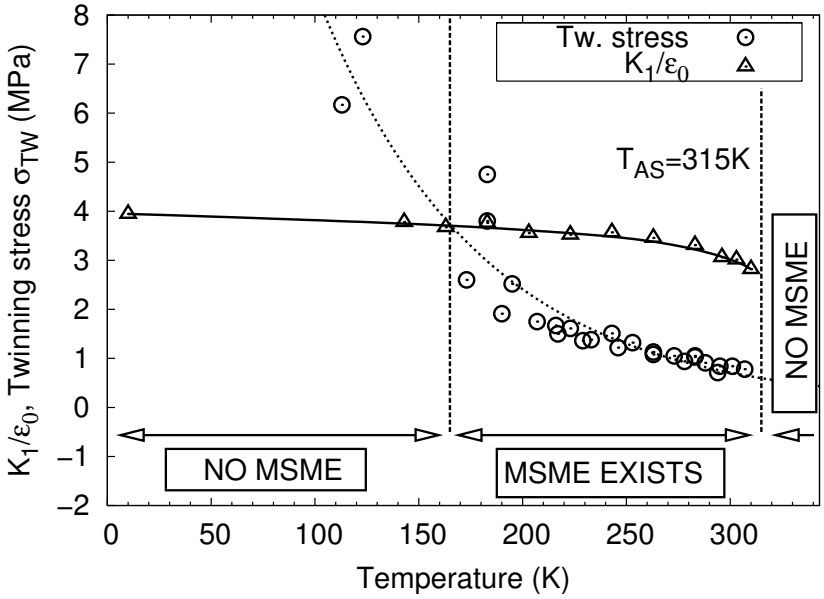

Figure 16: Determination of the limits for MSME in $Ni_{49.7}Mn_{29.1}Ga_{21.2}$ MSM alloy. No MSME can be observed below the temperature at which twinning stress (circles) exceeds the maximum possible magnetic stress K_1/ε_0 (triangles). Transformation to austenite at 315 K imposes the ultimate high temperature limit above which no MSME can occur.

4.3.5 The temperature region of the existence of MSME

When temperature dependences of all three key parameters of the existence of MSME, i.e. $\varepsilon_0(T)$, $\sigma_{TW}(T)$ and $K_1(T)$, are known then the determination of the temperature region where MSME exists is relatively straightforward using Relationship 4 (Chapter 2.3). This is illustrated in Figure 16 (detailed discussion is present in Publication IV). The existence of MSME is limited by transformation of the structure to parental phase at 315 K (no MSME can occur in an austenite) and by the temperature region where twinning stress $\sigma_{TW}(T)$ exceeds the magnetic stress $K_1(T)/\varepsilon_0(T)$, i.e., below 165 K. Between 165 K and 315 K, the existence of MSME is predicted by the theoretical model. Existence of MSME in this temperature region and low temperature limit of MSME were confirmed by direct observations of MSME. Possible intermartensitic transformations at low temperatures may impose additional limits for the existence of MSME, this is not, however, the case of the studied alloy in which no intermartensitic transformations were detected till 10 K.

The rather low Curie temperature of the Ni-Mn-Ga alloys, typically $T_C \approx 375$ K, imposes additional complication when considering usage of MSM alloys at high temperatures. When approaching the Curie temperature from below, magnetic anisotropy decreases rapidly with increasing temperature [64], Chapter 6.4 in Ref. [66], Chapter 12.3 in Ref. [17]. That is why the driving force for MSME

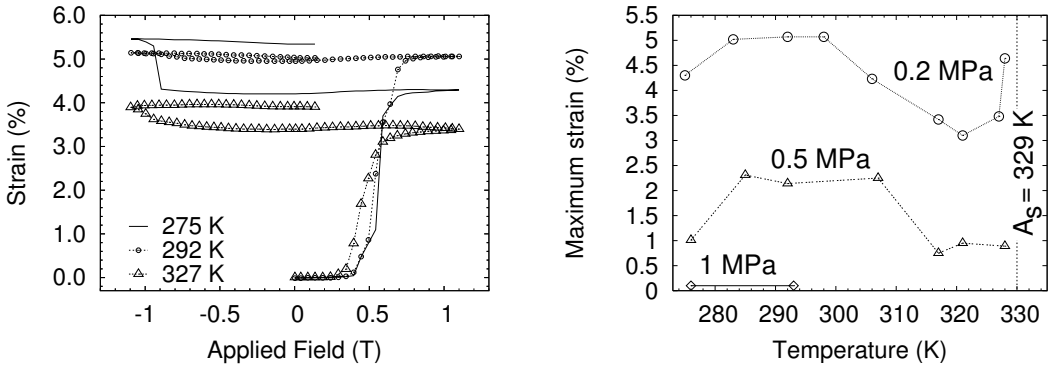

(a) (b)

Figure 17: Temperature dependence of maximum strain due to MSME in $Ni_{48.7}Mn_{29.1}Ga_{22.2}$ alloy. a) Examples of measurement in a quasistatic magnetic field at 0.2 MPa compressive stress at three different temperatures. Maximum strain is determined from the first magnetizing cycle as strain at maximum positive field with the martensite reorientation continuing, however, also during the second magnetizing cycle (negative field). b) Maximum strain as a function of temperature for three different compressive loads. Transformation to $L2_1$ parent phase at 329 K imposes the ultimate high temperature limit above which no MSME occurs.

(Equations 1 and 3 in Chapter 2.3) also decreases rapidly and from certain temperature $T < T_C$ the MSME may not occur. Nonetheless, transformation to austenite happens much earlier before this point has been reached for studied alloys, e.g. Figure 16. As discussed earlier in this Thesis the twinning stress and distortion of the lattice decrease with increasing temperature. This may compensate for the decreasing driving force. Above Curie temperature the alloy is paramagnetic, the driving force for MSME is zero and the MSME cannot occur. Some effort has been made to increase the Curie temperature by doping the Ni-Mn-Ga alloys by iron or by other metals [68, 69]. The highest temperature at which MSME was observed directly by the Author was 327 K on $Ni_{48.6}Mn_{29.2}Ga_{22.2}$ single crystal specimen with $A_S \approx 329$ K, Figure 17.

4.3.6 Conclusion

The temperature dependences of the key material parameters governing the existence of MSME were determined and used for investigation of temperature limits of MSME in $Ni_{49.7}Mn_{29.1}Ga_{21.2}$ alloy using the theoretical model. The magnetic stress K_1/ε_0 saturates at about 4 MPa at low temperatures while exponential-like increase of twinning stress with decreasing temperature was observed. Thus, the twinning stress is the main limiting factor for MSME at low temperatures. The limits determined using the model and limits determined by direct measurement of MSME agree well. It was

shown that the MSME exist in region approximately between 165 K to 315 K for studied $Ni_{49.7}Mn_{29.1}Ga_{21.2}$ alloy. The highest temperature at which MSME was observed directly by Author was 327 K on $Ni_{48.6}Mn_{29.2}Ga_{22.2}$ alloy. This limit was imposed by transformation of the alloy to austenite at 329 K. The demonstrated method of determining the temperature limits from material parameters using the theoretical model is general and can be used for any composition.

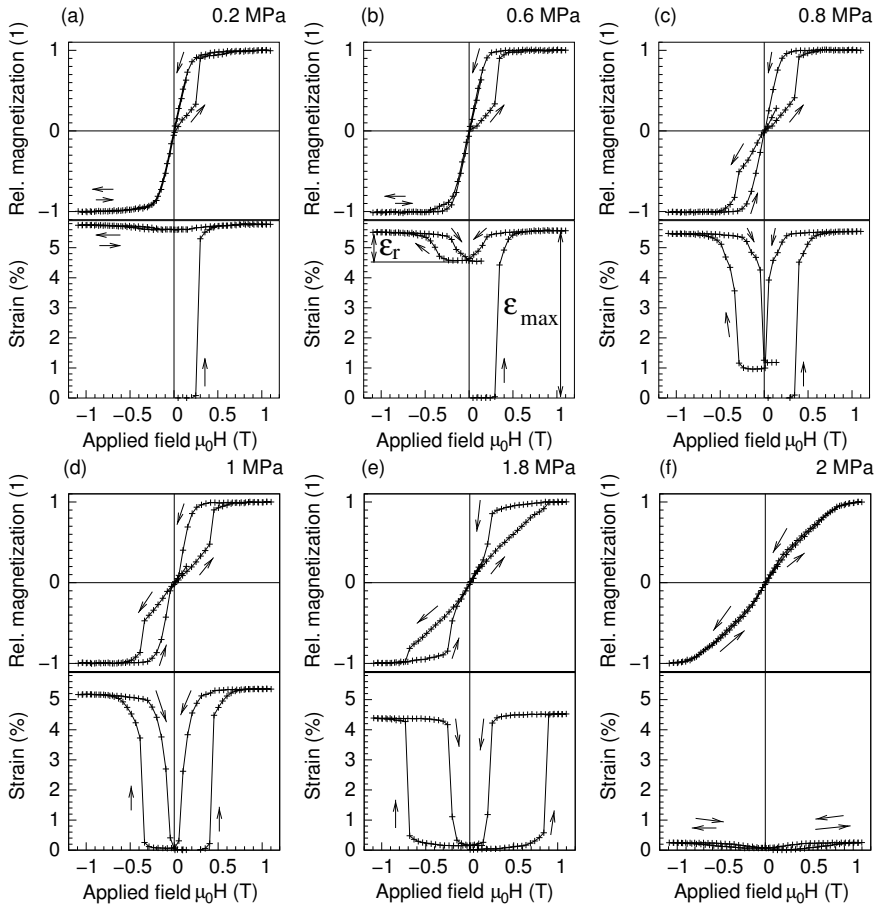

Figure 18: The effect of magnitude of external stress on the MSME for $Ni_{49.7}Mn_{29.1}Ga_{21.2}$ specimen with a very low twinning stress, $\sigma_{TW} = 0.8$ MPa, in quasistatic magnetic field. a) For small external stress, 0.2 MPa, $[001] \Rightarrow [100]$ reorientation along the external stress is observed, similarly as in Figures 9b and Figure 12a. b, c) For 0.6 MPa and 0.8 MPa stress partial reverse reorientation of the martensite ($[100] \Rightarrow [001]$ along the external stress) occurs additionally when magnetic field is decreased below certain level. Maximum strain (ε_{MAX}) and reversible strain (ε_r) are marked in (b). d, e) The reverse reorientation of the martensite is complete for external stress between 1.0 MPa and 1.8 MPa, which makes the MSME fully reversible and repeatable. The reverse reorientation of the martensite is reflected in the shape of magnetization curve, which is best visible in (e). Due to occurrence of the reorientation during the following magnetizing in negative field, the hysteresis is observed on magnetization curve also in the third quadrant. f) For external stress larger than 2 MPa MSME is almost completely suppressed.

4.4 Reversible MSME

This chapter discusses necessary conditions for reversible MSME and the reversible MSME is studied experimentally. Observed behavior is compared with the theoretical model.

4.4.1 Experimental observation of reversible MSME and associated changes of magnetization

To observe the MSME, Relationship 4 (Chapter 2.3), i.e. $K_1/\varepsilon_0 > \sigma_{TW} + \sigma_{EXT}$, must be satisfied. The K_1/ε_0 is typically about 3 MPa and twinning stress about 2 MPa in 5M martensite. Consequently, for compressive external stress lower than 1 MPa the MSME with about 6% macroscopic strain is observed as shown in Figure 9b for external stress of 0.2 MPa. After reorientation and removing of the field, martensite "remembers" its state, i.e. it remains reoriented. If the external stress is then increased above the twinning stress, martensite reorients back to the original state, which is accompanied by about -6% strain as demonstrated in Figure 9a.

It follows from the model that the two separate reorientations mentioned above can be combined into a single experiment with constant external stress provided that the condition

$$\frac{K_1}{\varepsilon_0} - \sigma_{TW} > \sigma_{EXT} > \sigma_{TW}. \tag{11}$$

is fulfilled. This is only possible for specimens with

$$\frac{K_1}{\varepsilon_0} > 2\sigma_{TW}, \tag{12}$$

i.e., for specimens with very low twinning stress (< 1.5 MPa for typical $K_1/\varepsilon_0 = 3$ MPa).

The Relationship 11 states that i)the maximum magnetic stress (K_1/ε_0) must overcome the sum of twinning stress and external stress (which facilitates the $[001] \Rightarrow [100]$ reorientation along the constant external stress when the magnetic field reaches a large enough magnitude) and ii) at the same time the constant external stress must be higher than the twinning stress (which facilitates the reverse reorientation, $[100] \Rightarrow [001]$ along the external stress, when the magnetic stress decreases below certain level). Experimental observation of such combined reorientation of a specimen with very low twinning stress for various magnitudes of constant external stress is shown in Figure 18. For constant external stress between 1 MPa and 1.8 MPa, fully reversible MSME is observed. I.e., the observed strain is close to 6% for every magnetizing cycle, not only for the first one as for usual (irreversible) MSME. The magnetization changes reflect changes of the arrangement of the martensite microstructure, and, thus, the reverse reorientation of the martensite during decreasing of magnetic field may be reflected in the shape of magnetization curve as is observed in Figure 18e (switching

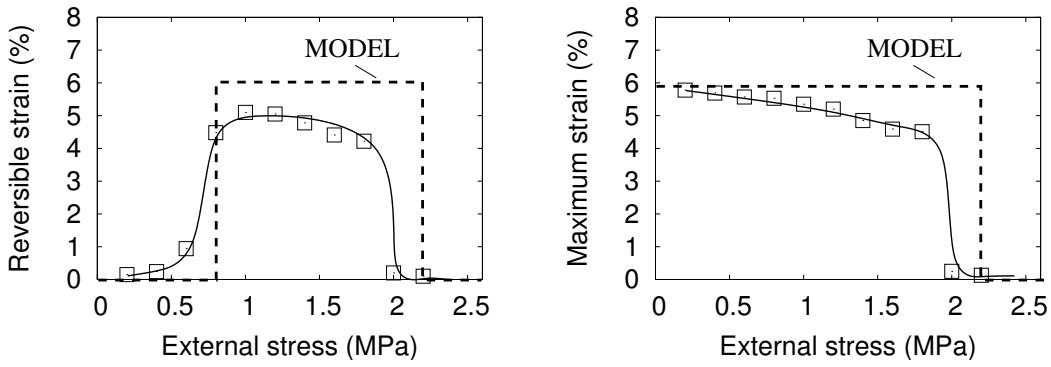

Figure 19: a) Magnitude of the reversible strain (squares) as a function of external stress and comparison with the model (dashed line). The solid line serves as guide for eyes. b) Magnitude of maximum strain (irreversible strain) as a function of external stress (squares) and comparison with the model (dashed line). The solid line serves as guide for eyes.

from easy to hard direction for near zero field). Due to occurrence of MSME during every magnetizing cycle, the hysteresis is observed on magnetization curve both in the first and the third quadrant, Figure 18c–e, not only in the first quadrant as for usual (irreversible) MSME, Figure 18a.

4.4.2 Modelling of reversible MSME

The reversible strain, ε_r, caused by a combined effect of magnetic field and external stress can be defined as the difference of the strain in a maximum field and the strain in a zero field in the second magnetizing cycle, as illustrated in Figure 18b. This strain will be close to zero for external stress lower than twinning stress and higher than $K_1/\varepsilon_0 - \sigma_{TW}$. Between these two limits a large reversible strain with magnitude close to distortion of the lattice will be observed. The maximum strain (irreversible strain, one-cycle strain) is obtained during the first magnetizing cycle, Figure 18b. The reversible and the maximum strain as functions of external stress determined from the measurement presented in Figure 18 are shown in Figure 19. Comparison with the used model (see above and Chapter 2.3) is further shown in Figure 19 using an experimentally determined $\sigma_{TW} = 0.8\,\text{MPa}$ and $K_1/\varepsilon_0 - \sigma_{TW} = 3.1 - 0.8\,\text{MPa} = 2.2\,\text{MPa}$ for the particular specimen. The agreement of experiment with the model is good considering that σ_{TW} was taken as constant for the whole deformation region.

The temperature dependence of the reversible strain was experimentally investigated and discussed within the same model in Publication VII. A 5–6% reversible strain was observed in temperature range 307–263 K which was in good agreement with the model.

4.4.3 Conclusion

The condition for existence of reversible MSME was formulated and reversible MSME with strain close to 6% was observed on a specimen fulfilling the condition. Temperature and stress dependences of reversible MSME were investigated, they are in good agreement with the theoretical model.

The experimental observations of changes of magnetization during reversible MSME demonstrate the close relation between the martensite microstructure and its magnetic properties. The presence of hysteresis in both the first and the third quadrant of magnetization curve is clear indication of reversible MSME.

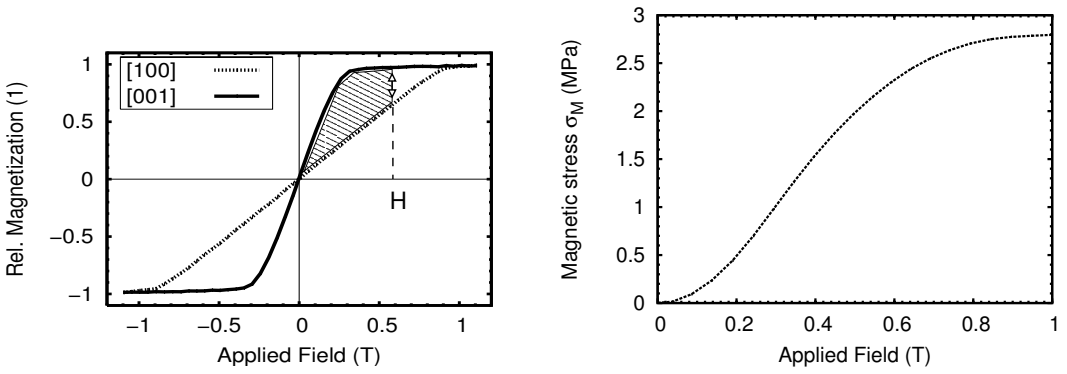

(a) (b)

Figure 20: a) The magnetic stress for a constant field H is determined from the area between magnetization curves measured for a single variant specimen with $[001]$ and $[100]$ directions along the field. The two measurements were done with the specimen in exactly the same position with only the orientations of martensitic variants (arrangement of martensite microstructure) being different. The specimen was constrained by 8 MPa external stress during measurement along $[100]$ direction to prevent MSME. The determined magnetization curves were not corrected for demagnetization. Thus, effects caused by the shape of a specimen are included in the determined magnetic stress. The changes of magnetization in the constant field H due to reorientation by stress are occurring along the line marked with arrows (see Chapter 4.6 for details). b) Determined magnetic stress as a function of applied field.

4.5 Magnetic field controlled superelasticity

This chapter describes extraordinary magneto-mechanical behavior of the MSM alloys in static magnetic field due to MSME, i.e. magnetic field controlled superelasticity.

4.5.1 Determination of magnetic stress

When a specimen located in a typical experimental arrangement (Chapter 3.3) is magnetized by magnetic field of a constant strength H, the magnetic stress can be stated according to Equation 1 (Chapter 2.3). It follows from the equation that the magnetic stress is proportional to the area between the measured magnetization curves of a single variant specimen as shown in Figure 20a. The dependence of magnetic stress on applied magnetic field is presented in Figure 20b.

4.5.2 Observation of magnetic field controlled superelasticity

When a single variant specimen exposed to a constant magnetic field is compressed by external stress, the motion of twin boundaries and reorientation of martensite occurs

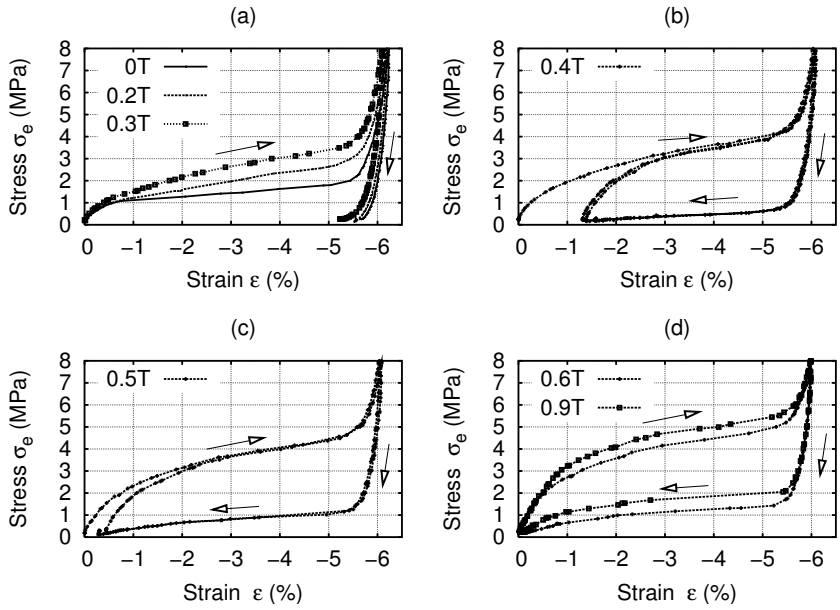

Figure 21: Stress-strain curves for $Ni_{49.7}Mn_{29.1}Ga_{21.2}$ specimen (5M martensite) in various constant magnetic fields. a) For a zero or a small field the reorientation occurs, but it is hindered by presence of the field b) Around 0.4 T the reorientation becomes partially reversible, but the stress needed for the reorientation increases further on. c,d) Further increase of the field results in full reversibility and further increase of the stress needed for the reorientation. The magnetic driving force is limited (max. K_1/ε_0), which is why increasing the magnetic field further above saturation field (0.9 T) has no effect (not shown).

for a large enough external stress. To obtain the deformation ε during $[100] \Rightarrow [001]$ reorientation along the stress, the external stress must equal the sum of magnetic stress $\sigma_M(H)$ and twinning stress $\sigma_{TW}(\varepsilon, H = 0)$. Both the twinning stress and magnetic field hinder the martensite reorientation during compression. Typically, magnetic stress is 3 MPa (in magnetic saturation) and twinning stress is about 2 MPa, and, thus, the stress necessary for reorientation in an applied field can be about two or three times higher (i.e. about 5 MPa) than in a zero field (given by value of twinning stress, i.e. 2 MPa).

There is almost no change in martensite microstructure (no reorientation of martensite) in a zero field during unloading, Figure 9a. But reverse reorientation of martensite ($[001] \Rightarrow [100]$ along the external stress) occurs in constant field with magnetic stress larger than the sum of twinning stress and external stress. If the magnetic stress is large enough, the reorientation will be complete.

To conclude the above, the presence of magnetic field increases the stress needed for reorientation of the martensite and it can make the reorientation reversible. Experimental observation of the effect of constant magnetic field on mechanical properties of $Ni_{49.7}Mn_{29.1}Ga_{21.2}$ specimen is shown in Figure 21. Similar was observed in

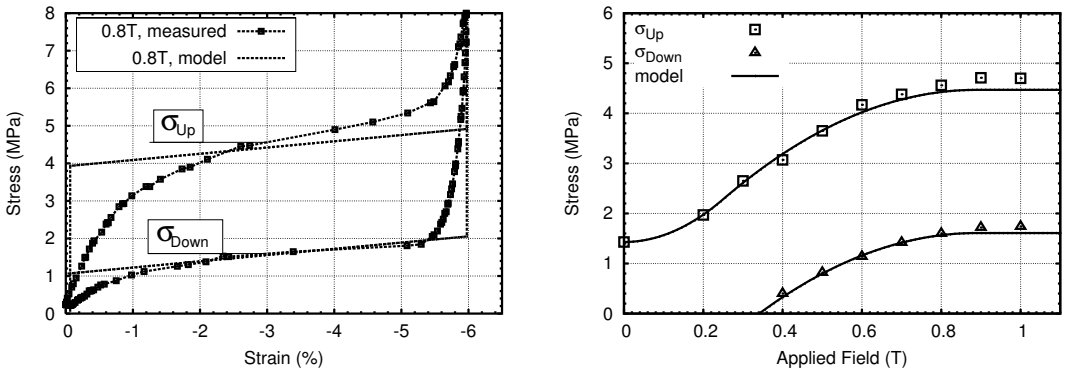

(a) (b)

Figure 22: a) Comparison of measured stress-strain curve and model calculation (solid line) for applied field 0.8 T. b) External stress necessary to induce strain of 3% (σ_{Up}, squares) during loading of specimen and stress induced by magnetic field at strain 3% (σ_{Down}, triangles) during unloading of specimen as functions of the applied field. Solid curves show calculation from the model.

Ref. [58]. The material behaves as superelastic due to MSME, and this superelasticity can be controlled by magnitude of magnetic field.

4.5.3 Modelling of the magnetic field controlled superelasticity

The experimental observations of the effect and its modelling are presented in Publication V. The model described in Chapter 2.3 is used in the publication. It predicts the behavior of a specimen in constant field based on the measured magnetization curves, determined magnetic stress (Figure 20b) and linearized twinning stress dependence. The model exhibits an excellent agreement with the experimental results as demonstrated in Figure 22a,b.

4.5.4 Partial cycles

An example of partial compressions of a specimen in 1 T magnetic field is shown in Figure 23. The area enclosed by the partial curves reflects work converted to heat during the given cycle. Due to this effective energy dissipation there is a considerable interest to utilize MSM materials for damping applications [70].

4.5.5 Conclusion

Magnetic field controlled superelasticity in Ni-Mn-Ga was demonstrated, experimentally studied and modelled. Good agreement with the theoretical model was obtained.

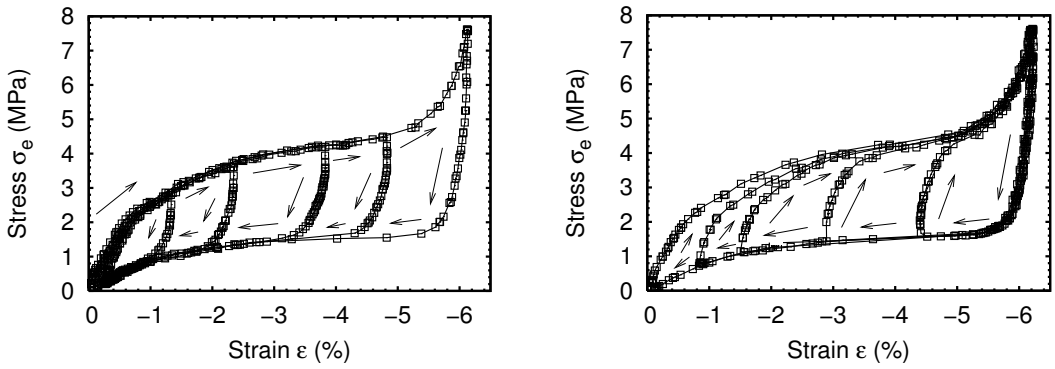

(a) (b)

Figure 23: Mechanical behavior of $Ni_{49.7}Mn_{29.1}Ga_{21.2}$ alloy (5M martensite) in 1 T static magnetic field, partial cycles. a) Loading and unloading between 0% and approximately 1%, 2%, 3.5%, 4.5%, 6% strain. b) Unloading and loading between -6% strain and approximately -4.5%, -3%, -1.5%, -1% strain.

4.6 Changes of magnetization during stress-induced reorientation

Since the changes of martensite microstructure and changes of magnetization are interrelated as shown in Figure 12, 18, one can expect that the magnetization of a specimen will change also during reorientation of the structure by mechanical stress in a constant magnetic field, Chapter 4.5. An example of an experimental observation of this effect is given in Figure 24. The hard axis ([100] direction) lies along the field at the maximum stress, while the easy axis ([001] direction) lies along the field at zero stress. This defines the limits for magnetization, which will be minimum at maximum stress and maximum at zero stress. These two points are located on the magnetization curves for [001] and [100] directions. Reorientation of the martensite moves the magnetization from the one point to the another as demonstrated by an arrow in Figure 20. Determination of the magnetization path with increasing degree of reorientation, i.e. $M(\varepsilon)$, for various magnetic fields was subject of Publication VI. The experimental results confirm correspondence of limiting points with the magnetization curves and show that the dependence is monotonous with a small hysteresis between $M(\varepsilon)$ for $[100] \Rightarrow [001]$ reorientation and $M(\varepsilon)$ for $[001] \Rightarrow [100]$ reorientation along the external stress (see also Figure 24). Nonetheless, the dependence is not linear as could be expected from superposition assumption, i.e. assuming that the total magnetization is given as the sum of magnetizations of individual variants. Although this is often assumed as well as observed experimentally to some extent, it is not exactly the case. If a thin lamella (band) of one variant is inside the other variant as e.g. in Figure 10e, the lamella has a large demagnetization field. On the other hand, when the lamella broadens, its demagnetization field decreases while demagnetization field of the vanishing lamellae increases.

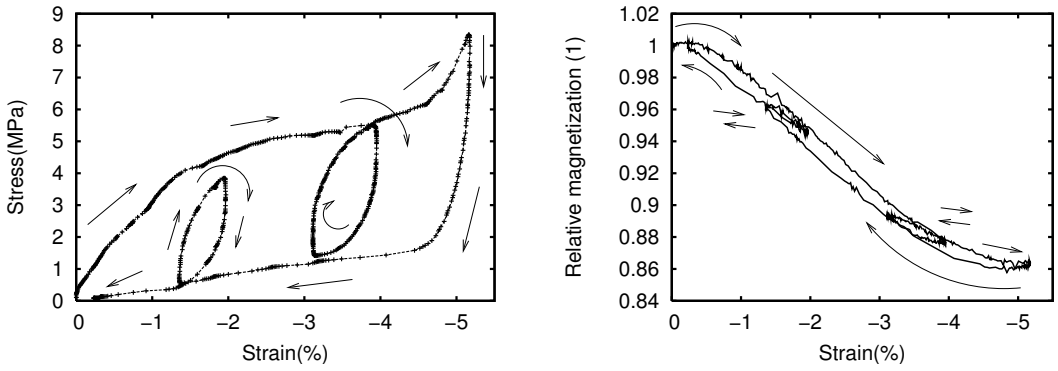

(a) (b)

Figure 24: Compression of $Ni_{48.5}Mn_{30.8}Ga_{20.7}$ specimen (5M martensite) in static 0.8 T magnetic field with partial cycles on loading and unloading. The stress was an independent variable, strain and magnetization were measured simultaneously. a) The stress-strain curve showing $[100] \Rightarrow [001] \Rightarrow [100]$ reorientation along external stress and partial cycles due to applied stress and MSME. b) The magnetization changes accompanying martensite reorientation, measured simultaneously with the stress-strain curve shown in (a).

Since the lamellae change their width during reorientation of the martensite, the demagnetization fields and magnetizations of the individual lamellae also change during the reorientation. This situation is obviously fairly complex and can be perhaps solved using a computer assisted numerical method but is very difficult to express analytically. Since there are only few lamellae in the specimen and their configuration and amount differs from alloy to alloy or even from specimen to specimen, the actual $M(\varepsilon)$ dependency might be individual for each of the specimens observed. The limiting points of magnetization at the zero and maximum strains are, however, clearly defined.

In addition to demagnetization effects of the lamellae, the observed nonlinearity of the stress-magnetization curves and their hysteresis can be associated with elastic deformation of the 5M martensite. The martensite has Young's modulus $E \approx 10\,\mathrm{GPa}$, determined from the slope of the stress-strain curve in the region of large stress after reorientation. Thus, during initial stage of loading, significant elastic straining occurs before the twin boundaries start moving. This strain lies within a range of $1\,\mathrm{MPa}/10\,\mathrm{GPa} = 0.1\,\%$. In the final stage of unloading the applied stress is much smaller than during the initial stage of loading, i.e. the elastic deformation is also proportionally smaller. Similar consideration can be applied for the region of maximum compression – elastic strain change of the amount of 0.1 %/MPa first occurs during release of the stress from its maximum. Only after that, the motion of the twin boundaries due to magnetic field occurs, which causes larger strains. The volume fraction of stress-induced variant present in the specimen is, therefore, different for loading

and unloading for the same strain. This is detected magnetically as the difference in magnitude of magnetization for the same strain and causes the hysteresis on the strain-magnetization curve as well as nonlinearities around the zero and maximum strains. The magnetization must, however, coincide for loading and unloading for zero strain, which is confirmed by our observation.

5 Conclusion

The main scientific contributions of the Thesis are summarized in the following list:

- Experimental apparatus for investigation of MSM alloys including unique MSM-apparatus suitable for measurement of magneto-mechanical properties of MSM alloys at various temperatures have been developed and built.
- Methods of preparation of single variant Ni-Mn-Ga specimen using external stress or magnetic field during martensitic transformation have been demonstrated and used successfully for preparation of single variant specimens. Possibility of training of specimens has been demonstrated.
- Temperature dependences of key material parameters determining existence of MSME have been obtained experimentally. The temperature dependences of magnetic anisotropy of Ni-Mn-Ga 5M and 7M martensites have been obtained for the first time. It has been shown for the first time that the twinning stress increase is exponential-like with decreasing temperature at low temperatures and that this increase is the main limiting factor for MSME existence at low temperatures (for 5M martensite).
- This Thesis presents the first attempt to explore experimentally and model the temperature limits of the MSME. It was shown that the temperature limits can be interpreted in the frame of the temperature dependence of the basic material constants of MSM alloys as twinning stress, magnetic anisotropy and distortion of the lattice.
- Experimental demonstration of various extraordinary magneto-mechanical effects in MSM alloys due to MSME, not discussed prior to this work, is presented in this Thesis. These effects are:
  - Fully reversible MSME with strain close to 6%. Condition of existence of fully reversible MSME was formulated and temperature and stress dependencies of reversible MSME were experimentally determined and discussed. Existence of the hysteresis on magnetization curve in the first and the third quadrant was shown and explained.
  - Magnetic field controlled superelasticity with strain close to 6%. The effect of magnetic field on superelastic behavior was experimentally determined and modelled.
  - Changes of net magnetization during loading of material in static magnetic field (local magnetization changes discussed previously in Ref. [20], changes of magnetization curves during loading discussed previously in Ref. [19]). Dependence on magnitude of static magnetic field was investigated and discussed.

- Unique simultaneous measurements of strain and magnetization during MSME, during reversible MSME, during loading of material in static magnetic field, and during martensitic and reverse transformation are presented in this Thesis. These measurements demonstrate and confirm close relation between martensite microstructure and its magnetic properties and corroborate that MSME is due to rearrangement of martensite microstructure.

- Good agreement of the presented experiment and the theoretical model supports its validity and demonstrates that this model is suitable for predicting various aspects of MSME such as temperature limits, reversible behavior and magnetic-field induced superelasticity.

- Some of the presented experiments can serve as application examples and may be inspiring for practical usage of the material.

References

[1] G. B. Olson, W. S. Owen (Editor), "Martensite", ASM International (1992), ISBN: 087170434X.

[2] K. Ullakko, J. K. Huang, C. Kanter, R. C. O'Handley, V. V. Kokorin, "Large magnetic-field-induced strains in Ni_2MnGa alloys, Appl. Phys. Lett. 69 (1996) 1966.

[3] A. A. Likhachev, K. Ullakko, "Magnetic-field-controlled twin boundaries motion and giant magneto-mechanical effects in Ni-Mn-Ga shape memory alloy", Phys. Lett. A 275 (2000) 142.

[4] S. J. Murray, M. Marioni, S. M. Allen, R. C. O'Handley, T. A. Lograsso, "6% magnetic-field-induced strain by twin boundary motion in ferromagnetic Ni-Mn-Ga", Applied Physics Letters 77 (2000) 886.

[5] O. Heczko, A. Sozinov, K. Ullakko, "Giant field-induced reversible linear strain in magnetic shape memory NiMnGa at room temperature", IEEE Transactions on Magnetics 36 (2000) 3266.

[6] R. D. James, R. Tickle, M. Wutig, "Large field-induced strains in ferromagnetic shape memory materials", Mat. Sci. Eng. A 273–275 (1999) 320.

[7] A. Sozinov, A. A. Likhachev, N. Lanska, K. Ullakko, "Giant magnetic-field-induced strain in NiMnGa seven-layered martensitic phase" Applied Physics Letters 80 (2002) 1746.

[8] P. Müllner, V. A. Chernenko, G. Kostorz, "Large cyclic magnetic-field-induced deformation in orthorhombic (14M) Ni-Mn-Ga martensite", Journal of Applied Physics 95 (2004) 1531.

[9] Outi Söderberg, "Novel Ni-Mn-Ga alloys and their magnetic shape memory behaviour", Doctoral dissertation, Picaset Oy (2004) Helsinki, ISBN 951-22-7415-9.

[10] O. Söderberg, Y. Ge, A. Sozinov, S.–P. Hannula, V. K. Lindroos, "Recent breakthrough development of the magnetic shape memory effect in Ni-Mn-Ga alloys", Smart Mater. Struct. 14 (2005) S223.

[11] G. H. Wu, W. H. Wang, J. L. Chen, L. Ao, Z. H. Liu, W. S. Zhan, T. Liang, H. B. Xu, "Magnetic properties and shape memory of Fe-doped $Ni_{52}Mn_{24}Ga_{24}$ single crystals", Applied Physics Letters 80 (2002) 634.

[12] R. D. James, M. Wuttig, "Magnetostriction of martensite", Philosophical Mag. A 77, (1998) 1273.

[13] A. N. Lavrov, S. Komiya, Y. Ando, "Antiferromagnets: Magnetic shape-memory effects in a crystal", Nature 418 (2002) 385.

[14] J. Enkovaara, O. Heczko, A. Ayuela, R. M. Nieminen, "Coexistence of ferromagnetic and antiferromagnetic order in Mn-doped Ni_2MnGa", Phys. Rev. B 67, (2003) 212405.

[15] R. C. O'Handley, S. M. Allen, "Shape memory alloys, magnetically activated ferromagnetic shape memory materials", Encyclopedia of Smart Materials, editor M. Schwartz (New York: Wiley) 936.

[16] Buschow J. (editor), O. Söderberg, A. Sozinov and V.K. Lindroos, "Giant Magnetostrictive Materials" The Encyclopedia of Materials: Science and Technology, Elsevier Science, 2004. In press.

[17] Sóshin Chikazumi, "Physics of Ferromagnetism", Second edition, Clarendon Press, Oxford (1997) ISBN 0198517769.

[18] H. H. Liebermann, C. D. Graham Jr., "Plastic and magnetoplastic deformation of Dy single crystals", Acta Mettalurgica 25 (1977) 715.

[19] Suorsa I, Tellinen J, Pagounis E, Aaltio I, Ullakko K., "Applications of magnetic shape memory actuators", Eighth International Conference on New Actuators, Bremen, Germany, Proceedings Actuator 2002 (2002) 158.

[20] Müllner P, Chernenko VA, Kostorz G., "Stress-induced twin rearrangement resulting in change of magnetization in a Ni-Mn-Ga ferromagnetic martensite", Scripta Mater 49 (2003) 129.

[21] C. P. Henry, J. Feuchtwanger, D. Bono, M. Marioni, P. G. Tello, M. Richard M, S. M. Allen, R. C. O'Handley, "AC performance and modeling of ferromagnetic shape memory actuators" Proc. SPIE 4333 (2001) 151.

[22] J. Tellinen ,I. Suorsa, A. Jääskeläinen,I. Aaltio, K. Ullako, "Basic properties of magnetic shape memory actuators", Eighth International Conference on New Actuators, Bremen, Germany, Proceedings Actuator 2002 (2002) 566.

[23] M. A. Marioni , R. C. O'Handley, S. M. Allen "Pulsed magnetic field-induced actuation of Ni-Mn-Ga single crystals", Appl. Phys. Lett. 83 (2003) 3966.

[24] C. P. Henry, P. G. Tello,D. Bono, J. Hong, R. Wagner, J. Dai, S. M. Allen, R. C. O'Handley, "Frequency response of single-crystal Ni-Mn-Ga FSMAs", Proc. SPIE 5053 (2003) 207.

[25] http://www.adaptamat.com/

[26] Carolyn Yeates, "Are Smart Materials Intelligent?" INSPEC Matters 77 (1994) 3.

[27] O. Söderberg, Y. Ge, I. Aaltio, O. Heczko, and S.-P. Hannula, "Ni-Mn-Ga multifunctional compounds", ESOMAT 2006 (Sept. 10-15, 2006), Bochum/Germany

[28] P. G. Tello, F. J. Castaño, R. C. O'Handley, S. M. Allen, M. Esteve, F. Castaño, A. Labarta, X. Batlle, "Ni-Mn-Ga thin films produced by pulsed laser deposition", Journal of Applied Physics 91 (2002) 8234.

[29] M. Landa, private communication.

[30] A. A. Likhachev, K. Ullakko, "Quantitative model of large magnetostrain effect in ferromagnetic shape memory alloys", Eur. Phys. J. B 14 (2000) 263.

[31] Y. Ma, S. Awaji, K. Watanabe, M. Matsumoto, N. Kobayashi, "X-ray diffraction study of the structural phase transition of Ni_2MnGa alloys in high magnetic fields", Solid State Communications 113 (2000) 671.

[32] P. J. Brown, J. Crangle, T. Kanomata, M. Matsumoto, K.-U. Neumann, B. Ouladdiaf, K R. A. Ziebeck, "The crystal structure and phase transitions of the magnetic shape memory compound Ni_2MnGa", J. Phys.: Condens. Matter 14 (2002) 10159.

[33] N. Lanska, O. Söderberg, A. Sozinov, Y. Ge, K. Ullakko, V. K. Lindroos,"Composition and temperature dependence of the crystal structure of Ni-Mn-Ga alloys", Journal of Applied Physics 95 (2004) 8074.

[34] X. Jin, M. Marioni, D. Bono, S. M. Allen, R. C. O'Handley, T. Y. Hsu, "Empirical mapping of Ni-Mn-Ga properties with composition and valence electron concentration", J. Appl. Phys. 91 (2002) 8222.

[35] V. V. Martynov, V. V. Kokorin, "The crystal structure of thermally- and stress-induced Martensites in Ni_2MnGa single crystals", J. Phys. III France 2 (1992) 739.

[36] J. Pons, V. A. Chernenko, R. Santamarta, E. Cesari, "Crystal structure of martensitic phases in Ni-Mn-Ga shape memory alloys", Acta Mater. 48 (2000) 3027.

[37] A. Sozinov, A. A. Likhachev, K. Ullakko, "Crystal structures and magnetic anisotropy properties of Ni-Mn-Ga martensitic phases with giant magnetic-field-induced strain", IEEE Transactions on Magnetics 38 (2002) 2814.

[38] Q. Pan, R. D. James, "Micromagnetic study of NiMnGa under applied field", Journal of Applied Physics 87 (2000) 4702.

[39] A. Sozinov, A. A. Likhachev, N. Lanska, O. Söderberg, K. Koho, K. Ullakko, V. K. Lindroos, "Stress-induced variant rearrangement in Ni-Mn-Ga single crystals with nonlayered tetragonal martensitic structure", J. Phys. IV France 115 (2004) 121.

[40] O. Söderberg, L. Straka, V. Novák, O. Heczko, S.-P. Hannula, V.K. Lindroos, "Tensile/compressive behaviour of non-layered tetragonal $Ni_{52.8}Mn_{25.7}Ga_{21.5}$ alloy", Mat. Sci. Eng. A. 386 (2004) 27.

[41] J. Kiang and L. Tong, "Modelling of magneto-mechanical behaviour of Ni-Mn-Ga single crytals" Journal of Magnetism and Magnetic Materials 292 (2006) 394.

[42] A. A. Likhachev, A. Sozinov, K. Ullakko, "Influence of external stress on the reversibility of magnetic-field-controlled shape memory effect in Ni-Mn-Ga", Proc. SPIE Vol. 4333 (2001) 197.

[43] O. Heczko, N. Lanska, O. Söderberg, K. Ullakko, "Temperature variation of structure and magnetic properties of Ni-Mn-Ga magnetic shape memory alloys", Journal of Magnetism and Magnetic Materials 242-245 (2002) 1446.

[44] M. I. Youssif, A. A. Bahgat, I. A. Ali, "AC Magnetic Susceptibility Technique for the Characterization of High Temperature Superconductors", Egypt. J. Sol. 23 (2000) 231.

[45] A. Zieba, S. Foner, "Detection coil, sensitivity function, and sample geometry effects for vibrating sample magnetometer", Rev. Sci. Instrum. 53 (1982) 1344.

[46] A. Niazi, P. Podar, A. K. Rastogi, "A precission, low-cost vibrating sample magnetometer", Current Science 79 (2000) 99.

[47] Foner, "Versatile and Sensitive Vibrating-Sample Magnetometer", Rev. Sci. Instrum. 30 (1959) 548.

[48] O. Heczko, L. Straka, "Magnetic properties of stress-induced martensite and martensitic transformation in Ni-Mn-Ga magnetic shape memory alloy", Mat. Sci. Eng. A 378 (2004) 394.

[49] A. Hakola , O. Heczko, A. Jaakkola, T. Kajava, K. Ullakko, "Pulsed laser deposition of Ni-Mn-Ga thin films on silicon", Applied Physics A: Materials Science & Processing 79 (2004) 1505.

[50] D. O. Smith, "Development of Vibrating-Coil Magnetometer", The Review of Scientific Instruments 27 (1956) 261.

[51] N. Glavatska, G. Mogilniy, I. Glavatskiy, S. Danilkin, D. Hohlwein, O. Sö derberg, V. K. Lindroos, A. Beskrovnij, "Temperature dependence of martensite structure and its effect on magnetic-field-induced strain in Ni_2MnGa magnetic shape memory alloys" J. Phys. IV France 112 (2003) 963.

[52] R. Tickle, R. D. James, T. Shield, M. Wuttig, V. V. Kokorin, "Ferromagnetic shape memory in the NiMnGa system", IEEE Transactions on Magnetics 35, (1999) 4301.

[53] O. Heczko, V. L'vov, L. Straka and S. P. Hannula, "Magnetic indication of the stress-induced martensitic transformation in ferromagnetic Ni-Mn-Ga alloy", J. Mag. Mag. Mat. 302 (2006) 387 .

[54] O. Heczko, K. Jurek, K. Ullakko, "Magnetic properties and domain structure of magnetic shape memory Ni-Mn-Ga alloy", J. Mag. Mag. Mat. 226-230 (2001) 996.

[55] K. Koho, J. Vimpari, L. Straka, O. Heczko, N. Lanska, O. Söderberg, K. Ullakko, and V.K. Lindroos, "Behaviour of Ni-Mn-Ga alloys under mechanical stress", J. Phys. IV France 112 (2003) 943.

[56] N. Glavatska, G. Mogylny, I. Glavatskiy, V. Gavriljuk, "Temperature stability of martensite and magnetic field induced strain in Ni-Mn-Ga", Scripta Materialia 46 (2002) 605.

[57] A. Sozinov, A.A. Likhachev, N. Lanska, O. Söderberg, K. Ullakko, V.K. Lindroos, "Stress- and magnetic-field-induced variant rearrangement in Ni-Mn-Ga single crystals with seven-layered martensitic structure", Materials Science and Engineering A 378 (2004) 399.

[58] V. A. Chernenko, V. A. L'vov, P. Müllner and G. Kostorz, T. Takagi "Magnetic-field-induced superelasticity of ferromagnetic thermoelastic martensites: Experiment and modeling", Phys. Rev. B 69 (2004) 134410.

[59] M. Pasquale, C. P. Sasso, G. Bertotti, V. L'vov, V. Chernenko, A. De Simone, "Analysis of mechanical and magnetic instabilities in Ni-Mn-Ga single crystals", Journal of Applied Physics 93 (2003) 8641.

[60] R. C. O'Handley, S. J. Murray, M. Marioni,H. Nembach, S. M. Allen, "Phenomenology of giant magnetic-field-induced strain in ferromagnetic shape-memory materials", Journal of Applied physics 87 (2000) 4712.

[61] F. Albertini, L. Pareti, A. Paoluzi, L. Morellon, P. A. Algarabel, M. R. Ibarra, L. Righi, "Composition and temperature dependence of the magnetocrystalline anisotropy in $Ni_{2+x}Mn_{1+y}Ga_{1+z}$ $(x+y+z=0)$ Heusler alloys", Applied physics letters 81 (2002) 4032.

[62] O. Heczko, K. Ullakko, "Effect of temperature on magnetic properties of Ni-Mn-Ga magnetic shape memory", IEEE transactions on magnetics 37 (2001) 2672.

[63] O. Heczko and L. Straka, "Compositional dependence of structure, magnetization and magnetic anisotropy in Ni-Mn-Ga magnetic shape memory alloys", J. Magn. Mag. Mat. 272-276 (2004) 2045.

[64] L. Straka and O. Heczko, "Magnetic anisotropy in Ni-Mn-Ga martensites", J. Appl. Phys. 93 (2003) 8636.

[65] H. Zijlstra, "Experimental Methods in Magnetism, 2. Measurement of Magnetic Quantities", North-Holland Publishing Company–Amsterdam (1967).

[66] R. C. O'Handley, "Modern Magnetic Materials: Principles and Applications", Wiley-Interscience (1999), ISBN: 0471155667.

[67] V. A. Chernenko, V. A. L'vov, V. V. Khovailo, T. Takagi, T. Kanomata, T. Suzuki, R. Kainuma, "Interdependence between the magnetic properties and lattice parameters of Ni-Mn-Ga martensite", J. Phys.: Condens. Matter 16 (2004) 8345.

[68] K. Koho, O. Söderberg, N. Lanska, Y. Ge, X. Liu, L. Straka, J. Vimpari, O. Heczko, V.K. Lindroos, "Effect of the chemical composition to the martensitic transformation in Ni-Mn-Ga-Fe alloys", Mat. Sci. Eng. A 378 (2004) 384.

[69] S. Guo, Y. Zhang, B. Quan, J. Li, Y. Qi, X. Wang, "The effect of doped elements on the martensitic transformation in Ni-Mn-Ga magnetic shape memory alloy", Smart Mater. Struct. 14 (2005) S236.

[70] J. Feuchtwanger, S. Michael, J. Juang, D. Bono, R. C. O'Handley, S. M. Allen, C. Jenkins, J. Goldie, A. Berkowitz, "Energy absorption in Ni-Mn-Ga-polymer composites", Journal of Applied Physics 93 (2003) 8528.

[71] M. Wuttig, J. Li, C. Crasiunescu, "A new ferromagnetic shape memory alloy system", Scripta Materialia 44 (2001) 2393.

[72] Yossef Ezer, "Magnetic Shape Memory (MSM) Effect in Ni-Mn-Ga Alloy", Doctoral dissertation, Acta Polytechnica Scandinavica, Chemical Technology Series No. 288, Espoo (2002) ISBN 951-666-593-4.

[73] Ilkka Suorsa, "Performance and modelling of magnetic shape memory actuators and sensors", Doctoral dissertation, TKK Dissertations 4, Espoo (2005) ISBN 951-22-7644-5.

[74] Jussi Enkovaara, "Atomistic Simulations of Magnetic Shape Memory Alloys", Doctoral disertation, Dissertation 119, Espoo, Otamedia Oy (2003) ISBN 951-22-6313-0.

[75] O. Heczko, L. Straka, and K. Ullakko, "Relation between structure, magnetization process and magnetic shape memory effect of various martensites occurring in Ni-Mn-Ga alloys", J. Phys. IV France 112 (2003) 959.

[76] L. Straka, V. Novák, M. Landa, and O. Heczko, "Acoustic emission of Ni-Mn-Ga magnetic shape memory alloy in different straining modes", Mat. Sci. Eng. A. 374 (2004) 263.

[77] O. Heczko, L. Straka, "Giant magnetic field induced strain - magnetic shape memory effect", Czechoslovak Journal of Physics 54, suppl. D (2004) D611.

[78] L. Straka, O. Heczko, "Reversible 6% strain of Ni-Mn-Ga martensite using opposing external stress in static and variable magnetic field", J. of Mag. Mag. Mat. 290-291 (2005) 829.

[79] O. Heczko, L. Straka, "Determination of ordinary magnetostriction in Ni-Mn-Ga magnetic shape memory alloy", J. of Mag. Mag. Mat. 290-291 (2005) 846-849 .

[80] O. Heczko, L. Straka, O. Söderberg, and S.P. Hannula, "Magnetic shape memory fatigue", Proceedings of the SPIE 5761 (2005) 513.

[81] O. Heczko, L. Straka, and S.-P. Hannula, "Stress dependence of magnetic shape memory effect and its model", Materials Science and Engineering: A 438-440 (2006) 1003.

[82] O. Heczko, L. Straka, I. Aaltio, and S.-P. Hannula, "Strain and concurrent magnetization changes in magnetic shape memory Ni-Mn-Ga single crystals - model", to be published.

Publications

I L. Straka, O. Heczko, V. Novák, and N. Lanska, **Study of Austenite-Martensite Transformation in Ni-Mn-Ga Magnetic Shape Memory Alloy**, Journal de Physique IV France 112 (2003) pp. 911–915.
Reused with permission from EDP Sciences. © 2003, EDP Sciences.

II O. Heczko, L. Straka, N. Lanska, K. Ullakko, and J. Enkovaara, **Temperature Dependence of Magnetic Anisotropy in Ni-Mn-Ga Alloy Exhibiting Giant Field-induced Strain**, Journal of Applied Physics 91 (2002) 8228–8230.
Reused with permission from Oleg Heczko, Ladislav Straka, Natalyia Lanska, Kari Ullakko, and Jussi Enkovaara, Journal of Applied Physics, 91, 8228 (2002). Copyright 2002, American Institute of Physics.

III L. Straka and O. Heczko, **Investigation of Magnetic Anisotropy of Ni-Mn-Ga Seven-layered Orthorhombic Martensite**, Journal of Magnetism and Magnetic Materials 272–276 (2004) 2049–2050.
Reused with permission from Elsevier. © 2004 Elsevier B.V.

IV O. Heczko and L. Straka, **Temperature Dependence and Temperature Limits of Magnetic Shape Memory Effect**, Journal of Applied Physics 94 (2003) 7139–7143.
Reused with permission from Oleg Heczko and Ladislav Straka, Journal of Applied Physics, 94, 7139 (2003). Copyright 2003, American Institute of Physics.

V L. Straka and O. Heczko, **Superelastic Response of Ni-Mn-Ga Martensite in Magnetic Fields and a Simple Model**, IEEE Transactions on Magnetics 39 (2003) 3402–3404.
© 2003 IEEE. Reprinted, with permission, from Ladislav Straka and Oleg Heczko, IEEE Transactions on Magnetics 39 (2003) 3402–3404.

VI L. Straka, O. Heczko, **Magnetization Changes in Ni-Mn-Ga Magnetic Shape Memory Single Crystal During Compressive Stress Reorientation**, Scripta Materialia 54 (2006) 1549–1552.
Reused with permission from Elsevier. © 2006, Acta Materialia Inc.

VII L. Straka, O. Heczko, S.–P. Hannula, **Temperature Dependence of Reversible Field-induced Strain in Ni-Mn-Ga Single Crystal**, Scripta Materialia 54 (2006) 1497–1500.
Reused with permission from Elsevier. © 2006, Acta Materialia Inc.

ISBN 978-951-22-8819-9
ISBN 978-951-22-8820-5 (PDF)
ISSN 1795-2239
ISSN 1795-4584 (PDF)